Physico-chemical and rheological analysis to understand the importance of root mucilage in mung bean (Vigna radiata) root-soil interactions

Moumita Sasmal
Abhijit P. Deshpande
Susy Varughese
susy@iitm.ac.in

Indian Institute of Technology Madras https://orcid.org/0000-0002-3092-1586

Research Article

Keywords: Mung bean, Root mucilage, Root-soil interactions, Nitrogen fixing, Rheology

Posted Date: May 6th, 2026

DOI: https://doi.org/10.21203/rs.3.rs-9073775/v1

Physico-chemical and rheological analysis to understand the importance of root mucilage in mung bean (*Vigna radiata*) root-soil interactions

Moumita Sasmal, Abhijit P. Deshpande, Susy Varughese

*Department of Chemical Engineering, Indian Institute of Technology Madras, Chennai, 600036, Tamil nadu, India.

*Corresponding author(s). E-mail(s): susy@iitm.ac.in;
Contributing authors: moumitasasmal0617@gmail.com;
abhijit@iitm.ac.in;

Abstract

Background and Aims: The importance of mucilage in root-soil interactions and during dry-wet cycles in plant growth is well known. This study aims at understanding the role of fresh root mucilage in nitrogen fixation, drought tolerance, and root-soil interactions from physio-chemical properties, composition, wettability, and flow behaviour using novel approaches. Important legume crop, Mung bean (*Vigna radiata*) is used as the model species.

Methods: Fresh root mucilage collected from axenically grown Mung bean seedlings is studied for chemical composition, rheological behaviour, wettability and root-soil interactions. Root-soil interactions under wet and dry conditions are probed using soil blobs formed on live root tips under different conditions.

Results: Chemical analysis of fresh mung bean root mucilage shows that it is rich in pentose sugars which facilitates the biological nitrogen fixation by the roots. Rheological study indicates the gel-forming ability of the mucilage arising from pectic polymer networks of homogalacturonan (HG) and rhamnogalacturonan-I (RG-I) domains. Root-soil interactions inferred from image analysis of root-mucilage-soil blobs and supported by flow/wettability studies show strong correlation with viscoelasticity and surface tension characteristics of fresh mucilage.

Conclusion: Mung bean root mucilage, rich in pentose sugars gives strong evidence for the exclusive symbiotic relationship between the mung bean and the root nodule microbe, Bradyrhizobium. Mucilage is found to withstand temperature fluctuations in the soil without structural changes indicating suitability for drought tolerance. The weak gel-like behaviour along with yield stress and shear

thinning characteristics supports the hydration and lubrication ability during root growth involving shear forces under dry conditions.

Keywords: Mung bean, Root mucilage, Root-soil interactions, Nitrogen fixing, Rheology

1 Introduction

The interface between the plant root and nearby soil is significantly influenced by the mucilage secreted from the root [1, 2]. Mucilage, a polymeric gel, is exuded by the border cells of the plant root tip in response to physical stresses and mechanical restriction [3]. Root mucilage, consisting mainly of various high-molecular-weight polysaccharides, serves a variety of functions in the rhizosphere [4, 5]. The hydraulic and structural properties of the rhizosphere are regulated by the root mucilage, due to its specific physico-chemical characteristics [6, 7]. For example, the wetting and gel characteristics of the root mucilage, specifically surface tension and viscoelastic properties, play important roles in rhizosphere hydraulic processes. The surface tension and viscosity of these hydrogels resist the breaking of the capillary bridges formed between soil particles, which gradually contract during drying and eventually rupture as the drying continues [8]. The interfacial role of root mucilage in soil aggregate stability/structure [9–12]), soil anchorage [13], and soil wetting/dewetting characteristics in the hydrated and dry states of mucilage have been investigated in recent years [14–16]. Root mucilage is also reported to modify the rhizosphere by stabilising microbial and enzymatic activity [17–19]. Maize root mucilage, covering the root cap zone with a thickness varying between 50 and 1000 μm [20], has been investigated for viscosity, surface tension, and viscoelastic properties in a limited range of temperature and frequency [21–24]. In addition to the chemical composition, the mechanical and physical properties of the mucilage can alter the structural constitution and hydraulic properties of the rhizosphere [7, 25–27]. Root mucilage has higher viscosity than water due

to the high molecular weight polysaccharides present [6, 8, 24, 28, 29] and a lower surface tension due to the phospholipids present [16, 30, 31]. This lower surface tension and higher viscosity of root mucilage in comparison to water are expected to support the percolation of the gel-like mucilage through the soil pores within the rhizosphere during dry periods, which could also serve as a water reserve for plants [8]. Due to the swelling properties and the water retention capacity of the mucilage, the moisture content of the soil is found to increase around the roots of chickpea, white lupin, and maize, regardless of the water uptake by the roots [3, 32]. However, after a dry period, the immediate soil layer surrounding lupin plants experienced a slower rewetting, followed by a prominent increase in moisture content in contrast to that of the bulk soil [3]. This delay in rewetting was attributed to the phospholipids present in the root mucilage, which make the soil hydrophobic temporarily following a dry period [31]. However, after a short delay in rewetting, the water content in the soil increases again due to the capacity of the mucilage to re-swell even after repeated drying processes [33]. Maize and pea root mucilages have been studied for their frictional properties [34, 35], and wheat root mucilage for its physicochemical properties, soil stabilisation and Al accumulation [28, 36]. Analysis of the root mucilage from different species shows neutral and acidic polysaccharides as major components. In addition to this, smaller quantities of various monosachharides (fructose, arabinose, galactose, glucose, xylose, mannose, fructose, ribose, sucrose, etc) glyco and phospholipids, fatty acids, proteins, and amino acids (maize - [37]; maize - [38]; sorghum - [39]) present in the mucilage also play various functional roles in root-soil interactions [8, 16, 30, 31]. Among various plant species, cereals such as maize, wheat, and sorghum, and legumes such as chick pea and lupin have been widely used for root mucilage studies due to the ease of collection of mucilage and the global relevance to food security [40–44]. In addition to the cereals, legumes are important among worldwide agricultural produce due to their increasing relevance as sources of plant-based proteins. They also contribute to soil

fertility and environmental protection [45]. Mung bean (*Vigna radiata*) is an extensively studied legume that grows primarily in tropical regions characterized by dry or semi-arid conditions and temperatures between 27 and 30 °C [46]. Mung bean is found suitable for growing in well-drained loamy to sandy loam soil and is a drought-tolerant plant [47–49]. In this context, understanding the physico-chemical and mechanical properties of mung bean root mucilage and its role in root-soil interactions is highly relevant, especially due to the changing climate conditions.

In this work, we investigate root-soil interactions using approaches based on microstructural, physicochemical, and rheological characterization of freshly collected root mucilage. Soil blobs adhering to the mucilage-laden root tip are used as a novel approach to understand the role of mucilage in protecting the root tip from excessive drying. The mung bean is found to be a new and easy-to-grow source for fresh root mucilage studies, in addition to the existing limited number of plants in this category. The frequency and temperature-dependent rheological behaviour of fresh mucilage provides new insights into their visco-elastic gel-like behaviour and the thermal stress tolerance characteristics.

2 Methods and material

2.1 Materials

The seeds of organically grown mung bean or green gram (*Vigna radiata*) were purchased from 24 Mantra Organic (Sreshta Natural Bioproducts Ltd., Bidar, Karnataka, India). 30% H_2O_2 and 98% sulfuric acid (36 N) used to prepare the piranha solution were purchased from Thermo Fisher Scientific India Pvt Limited, Mumbai, and Merck Specialities Private Limited, Mumbai, India, respectively. 99% Trifluoracetic acid was purchased from Sigma-Aldrich (St. Louis, MO, USA). Low methoxy pectin (LM pectin) of citrus origin (galacturonic acid content, 87% and degree of esterification 39%) was purchased from Krishna Pectins, Jalgaon, Maharashtra, India. 0.01% (w/v)

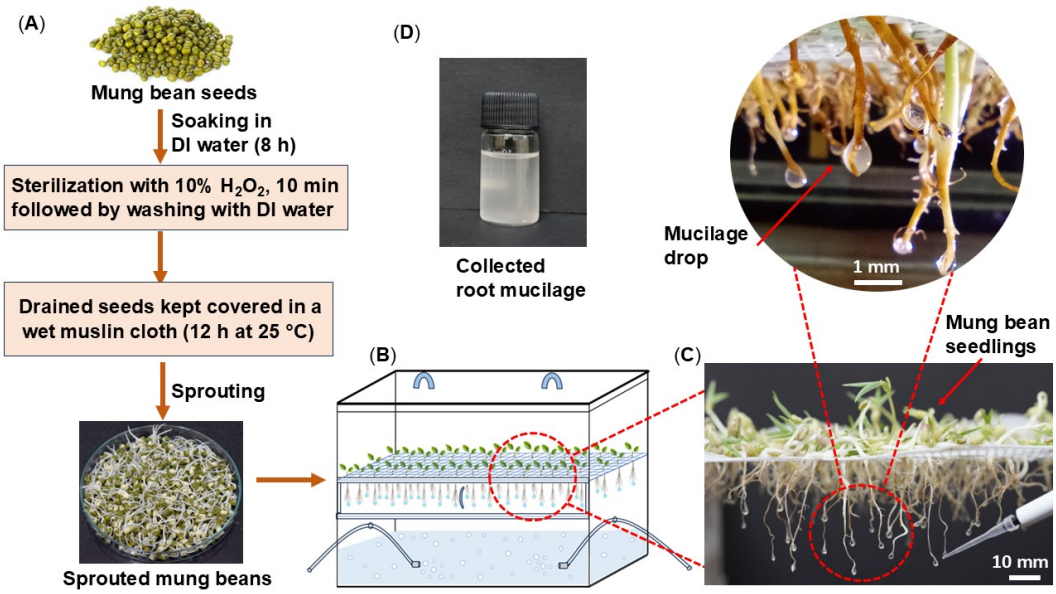

Fig. 1 Protocol for Mung bean (*Vigna radiata*) root mucilage collection. (A) Stepwise methodology for mung bean seed sprouting. Mung bean seeds were soaked in DI water for 8 h at room temperature (25 °C) for water imbibition. Swollen seeds were sterilized using 10% H_2O_2 followed by washing with deionised water. Excess water was drained from the seeds, and the seeds were kept covered in a wet muslin cloth for 12 h at 25 °C for sprouting. (B) Schematic showing the experimental box for mucilage exudation and collection from axenically grown seedlings. Mung bean sprouts were placed on a plastic mesh inside the humidity-controlled Perspex box. 72% RH was maintained inside this box by keeping water below without touching the root tips. (C) The seedlings are shown to grow axenically towards the water surface. The image shows 3-day-old seedlings with exuded mucilage at the root tips after exposure to the humidified conditions for 24 h. Mucilage drops formed at the root tip were collected using a micropipette by applying negative pressure. Each root tip exudes ∼3 μL. (D) Freshly collected root mucilage in the glass vial. The collected mucilage is translucent in appearance.

aqueous solutions of ruthenium red and methylene blue dyes were used for staining the mucilage. Calcium chloride ($CaCl_2.2H_2O$) and magnesium chloride ($MgCl_2.6H_2O$) used for cross-linking pectin were obtained from Merck Specialities Private Limited, Mumbai, India, and Sisco Research Laboratories Pvt. Ltd., Mumbai, India, respectively. Sandy loam and sandy clay loam soils (particle size < 310 μm) used for the soil-mucilage dry-wet cycle analysis were provided by the Soil Testing Laboratory, Tamil Nadu Agricultural University (TNAU), Kanchipuram, Tamil Nadu, India. The soil samples were dried in an air oven at 60 °C for 24 h. Deionised water from Millipore was used for preparing samples.

2.2 Collection of mucilage

Fresh mucilage was collected using the procedure described in Holz et al. [50] with modifications described herein (Fig. 1). Mung bean seeds were soaked in deionised water for 8 h, followed by a surface sterilization process by immersing in 10% H_2O_2 solution for 10 min. The sterilized seeds were kept tied inside a clean wet muslin cloth for 12 h at 25 °C for water imbibition and germination (Fig. 1A). The experimental set-up for growing the seedlings and collecting the root mucilage is shown in Fig. 1B. A PVC mesh with a 2 mm mesh size was mounted inside a $40 \times 30 \times 30$ cm perspex box. The box was partially filled with deionised water to a height of 10 cm, and two air stones connected to plastic tubes were placed at the bottom of the box. These plastic tubes were attached to a small aquarium pump. The air stones create a continuous flow of tiny bubbles inside the water. This increases the humidity inside the closed environment of the experimental box. The box was sealed with a lid to maintain a stable, high-humidity condition of 72% RH. The germinated mung bean seeds were placed on the PVC mesh for axenic growth of the seedlings. The roots of the plants grew downwards through the mesh as can be observed in Fig. 1C. Small drops of hydrated mucilage were formed around the root tips after 3 days in response to the high humidity inside the box. These mucilage drops from each root tip were carefully collected (Fig. 1D) once a day using a micro-pipette applying negative pressure. Each seedling exuded approximately 3 μL of fresh mucilage. Multiple seedlings were used to collect a sufficient amount of fresh mucilage. This mucilage was then utilized for subsequent experiments, including physicochemical characterization, rheology, and microscopy, as described in later sections. For FTIR, NMR, FT-Raman, and HPLC analysis, dried mucilage was used.

Total solid content (S) of the freshly collected mucilage was determined after vacuum drying at 25 °C and 50 mbar pressure. The mucilage sample was weighed every

30 min until the sample weight remained constant.

$$S = \frac{W_d}{W_w}, \tag{1}$$

where W_w and W_d are the initial (as collected) and final (as dried) weight of the mucilage. To compare the properties with fresh native mucilage, reconstituted mucilage was prepared by dissolving dry root mucilage powder in deionised water at 30 °C under sonication. Reconstituted mucilage 0.5, 0.7, 1, 2, and 4 mg/ml concentrations were prepared for various tests.

2.3 Preparation of pectin gels

LM pectin gels were used in this study to compare with the properties of the mucilage since pectin is a major polysaccharide in the mucilage composition. Pectin-Ca and pectin-Mg gels were prepared using LM pectin as detailed in [51]. LM pectin (0.35 wt%) was dissolved in deionised water by stirring for 18 h at 60 °C. Calcium chloride and magnesium chloride were used as crosslinking agents. The crosslinking ratio (R) relates the stochiometric concentration of calcium or magnesium ions to that of the non-methoxylated galacturonic acid content in the pectin. R is defined as,

$$R = \frac{2[Ca^{2+}]}{[COO^{-}]} \tag{2}$$

To obtain the pectin-Ca and pectin-Mg gels, required amounts of calcium chloride or magnesium chloride solution were added to the 0.35 wt% pectin solution drop by drop at 25-30 °C with stirring. This solution, stirred for 10 min was left undisturbed for 24 h at room temperature (25-30 °C) to complete the crosslinking process to obtain the gels. These gels were kept under ambient conditions and were used within 24 hours for further experiments.

2.4 Characterization of mucilage

2.4.1 Microstructure and morphology

Morphology of the fresh and dried root mucilage was studied using the Optical Microscope (Nikon - LV 100 ND, 100x magnification). Ruthenium red and methylene blue dyes were used for staining the pectin and the cellulose components present in the mucilage before optical microscopy was carried out. Scanning Electron Microscopy (SEM) studies were carried out using Field Emission Scanning Electron Microscope (FE-SEM) (Apreo S-SEM, US). For lyophilization, the root tip with mucilage was placed on a cover glass and lyophilized using a Scanvac lyophilizer (LaboGene, Denmark) under controlled conditions: initial freezing at -80 °C for 1 h, followed by drying at -96 °C for 24 h under a vacuum pressure of 0.1 mbar. The lyophilized root tip samples with mucilage were mounted on adhesive-coated aluminum stubs and sputter-coated with gold prior to the analysis. Elemental analysis of the mucilage was carried out along with SEM using energy-dispersive X-ray spectroscopy (EDX).

2.4.2 Drying, re-hydration ability and soil wetting characteristics

Drying and re-hydration behaviour of the fresh mung bean root mucilage was studied using an optical microscope (Nikon - LV 100 ND) at 100x magnification. The root tips, along with fresh mucilage, were placed on a clean glass slide and observed during the drying and rehydration process. Observations on drying and re-hydration of the mucilage along with the root tip were carried out by capturing optical images using a goniometer camera (Attension Theta Optical Goniometer, Biolin Scientific, Sweden). For this, root tips with fresh mucilage were suspended in air in front of the camera and allowed to dry at 25 °C and 60% RH. Images of the root tip with mucilage were collected at 5 min intervals. From the images, the diameter of the mucilage drop along with the root tip, at the mid-point, was estimated using ImageJ software. Similar studies were also carried out to understand root-soil interactions through mucilage. Root

tips with fresh mucilage were dipped in pre-dried sandy clay loam and sandy loam soil samples. These root tips were pulled out gently along with a soil blob adhering to them. The soil blobs were kept suspended in front of the Goniometer camera, and images were collected every 5 minutes while it was allowed to dry in air at 25 °C and 60% RH. The diameter of the soil blob at mid-point was estimated from the optical images using ImageJ software. Both the root tip with mucilage and the soil blobs were dried to an equilibrium state (no further changes in the diameter). To understand the re-hydration capability of the mucilage, 0.5 μL of deionised water was carefully introduced to the root tip (with dried mucilage) using a micropipette. Images were captured during the rehydration process until the drop reached equilibrium swelling (no further change in the diameter). The swollen samples were allowed to dry for a second cycle at 25 °C and 60% RH until the samples reached equilibrium drying. Images were captured every 5 minutes during these processes for changes in the diameter. To understand the effect of drying of mucilage and its capability to wet and adhere to the soil, another set of experiments was also conducted using root tips with mucilage dried to different extents and dipping them in clay loam soil. In this case, the images were collected immediately after dipping the root tip in the soil.

2.4.3 Physico-chemical characterization

FTIR spectra of vacuum-dried root mucilage powder and LM pectin powder were recorded in the range between 500 and 4000 cm^{-1} wave number at 4 cm^{-1} resolutions in the ATR-FTIR mode on a BRUKER Alpha spectrometer.

NMR analysis was carried out on dried mucilage using NMR Bruker AV III 500 MHz Spectrometer. During the experiments, the probe temperature was maintained at 298 K, and D_2O was used as the solvent.

FT-Raman Spectra were obtained for dried mucilage and LM pectin powder samples and Ca-crosslinked pectin (R=0.25) films using BRUKER RFS 27 MultiRAM

FT Raman Spectrometer with Nd-YAG laser 1064 nm source and LN2 LN2-cooled ultra-high sensitivity Ge detector.

High-performance liquid chromatography (HPLC) was carried out on root mucilage to obtain the monosaccharide composition using the protocol given in [52]. 20 mg of vacuum-dried mung bean root mucilage was hydrolyzed in 1.5 mL of 2 M TFA solution at 110 °C for 3 h. After cooling to room temperature, 1 mL of methanol was added to the mixture and dried at 70 °C under a stream of nitrogen to remove TFA. This process was repeated twice to ensure the complete removal of TFA. The dried residue was used for the analysis of monosaccharide composition. The obtained dried residue was resuspended in 1 mL of 5 mmol H_2SO_4 and passed through a 0.22 μm filter. 20 μL of this filtered solution was injected into a Shimadzu HPLC system (Shimadzu, Japan) equipped with a Rezex ROA-Organic Acid H^+ (8%) ion-exclusion column (250 mm $\times$ 4.6 mm, Phenomenex, USA), and a refractive index detector (Shimadzu). The analytical column was operated at 50 °C with 5 mmol H_2SO_4 as the mobile phase, and the mobile phase flow rate was 0.6 mL/min. The monosaccharide identification was performed by matching the retention times of the components in the root mucilage to those of authentic monosaccharide standards, each prepared at a concentration of 2 mg/mL (rhamnose, xylose, arabinose, galactose) in 5 mmol H_2SO_4 solution. HPLC of monosaccharide standards was run individually and as mixtures.

2.4.4 Surface tension and wetting characteristics

Surface tension using the pendant drop method and contact angle measurements using the sessile drop method were carried out on a Tensiometer (Attension Theta Optical Tensiometer, Biolin Scientific, Sweden, for 10 sec at 25 °C). Freshly collected mucilage, reconstituted mucilage of different concentrations, 0.35 wt% LM pectin solution, and deionised water were tested. Contact angles of freshly collected mucilage on glass and Teflon substrates were obtained. Prior to measuring the contact angle, glass slides

were cleaned using piranha solution (36 N sulfuric acid and 30% hydrogen peroxide in 3:1 ratio), and Teflon substrates were cleaned using deionised water.

2.4.5 Rheological characterization

Rheological behaviour of the root mucilage was studied on Anton Paar MCR-302e rheometer with a cone and plate geometry (plate diameter 25 mm). The gap was 0.047 mm, and shear rates were varied from 0.01 to 1000 s^{-1}. Steady shear experiments were carried out on freshly collected root mucilage of mung bean, pectin solution (0.35 wt%), pectin-Ca gel (0.35 wt%, R=0.25), and pectin-Mg gel (0.35 wt%, R=0.8). Reconstituted mucilage samples prepared in deionised water were also used for comparison. Small amplitude oscillatory shear (SAOS) tests were performed at angular frequency varying from 0.1 to 10 rad/s at a strain amplitude of 1% at 25 °C. Temperature stability of the mucilage was studied by conducting heating experiments from 5 °C to 50 °C, followed by cooling starting from 50 °C to 5 °C at 1% strain amplitude and angular frequency of 1 rad/s. These cycles were repeated 3 times.

3 Data reproducibility

Mung bean seedlings were grown axenically at a temperature of 25 °C and 72% RH to collect the root mucilage. The results reported here are based on multiple experiments repeated over a period of two years on multiple batches of mung bean seedlings grown from different batches of seeds. Although the solid content of the collected mucilage varied between 0.2 wt% and 0.4 wt% across different batches, for experiments involving fresh mucilage, such as rheology and surface tension, mucilage with a solid content of 0.4 wt% was used. All experiments were performed at least three times to ensure repeatability. The rheology and surface tension data presented here represent the average values with standard errors. Drying and re-hydration experiments were performed three times, with a representative graph presented.

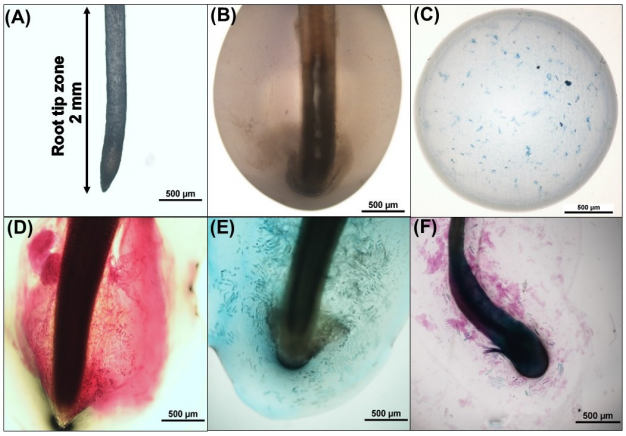

Fig. 2 Optical microscopy images of root tips of 3-day-old mung bean seedlings. (A) The root tip before exposure to humidity shows no mucilage exudation. (B) Root tip exposed to humidity (72 % RH for 24 h inside the experimental box) shows exuded mucilage on the root tip. (C) Drop of freshly collected root mucilage deposited on the cleaned glass slide. Methylene blue staining shows the cellulosic regions present in the mucilage, indicating the presence of border cells in the mucilage. (D) Ruthenium red staining showing pectin-rich regions of the mucilage. (E) Methylene blue staining showing cellulosic regions. (F) Exuded mucilage on the root tip, stained using ruthenium red and methylene blue simultaneously to show the distribution of pectin and cellulosic regions. Root border cells containing the cellulosic regions are visible in blue, while the pectin regions are visible in pink. Representative images are presented from three independent experiments. All images are at 5x magnification.

4 Results

The measured density of freshly collected mung bean root mucilage is 1.05 g/cm^3. The average solid content of the mucilage is 0.4 wt% or 4 mg/ml. The root growth rate for mung bean was measured by monitoring the increase in root length with time and was found to vary between 0.5-2 cm/day. In sandy loam and sandy clay loam soil, the growth rate was found to be 1-2 cm/day and 1-1.5 cm/day, respectively. The root growth rate for maize in sandy soil was reported as 1-4 cm/day [53]. Root growth rate was measured to estimate the shear rate experienced by the mucilage layer during root penetration in the soil. This shear rate is found to vary between 0.007 s^{-1} and 0.014 s^{-1} for mung bean.

4.1 Microstructure and morphology

Optical microscopy images of the root and the mucilage are shown in Fig. 2. The figure includes the images of the root without mucilage, the root with exuded mucilage, and stained mucilage. In the case of mung bean, the root mucilage exudation occurs in the root tip zone of approximately 2 mm length (2A). The mucilage drop diameter is approximately 0.7 mm (2B) at the centre. Figure 2C shows the collected mucilage stained using methylene blue to highlight the cellulosic regions. This image also shows that the collection procedure did not affect the mucilage composition. In Fig. 2D, the pink colour obtained using ruthenium red indicates the presence of acidic polysaccharides, such as pectin, in the mucilage. Methylene blue staining (Figs. 2C and 2E) shows the presence of cellulose in the mucilage originating from the root border cells. To identify the distribution of pectin and cellulosic components present in the mucilage, simultaneous staining using both ruthenium red and methylene blue was carried out and is shown in Fig. 2F. The surface morphology of the dried mucilage was examined using scanning electron microscopy (Fig. 3). The image in Fig. 3A shows the exuded mucilage layer on a 3-day-old mung bean root tip, dried on a glass slide. It shows the presence of numerous root border cells (BC) in the region (marked with white arrows) on the root tip surface near the root cap zone. From a close examination of the image, it can be observed that the loosely adhered peripheral border cells are embedded in a thin layer of mucilage (Fig. 3B). The morphology of the mucilage without the root border cells indicates a uniform distribution around the root tip (Fig. 3C). The elemental analysis conducted using energy-dispersive X-ray spectroscopy (EDS) along with SEM analysis shows the presence of not only divalent ions, such as, Ca^{2+} and Mg^{2+}, but also the presence of monovalent ions, such as, K^{+} in the mucilage (Fig. 3D).

4.2 Physico-chemical characteristics

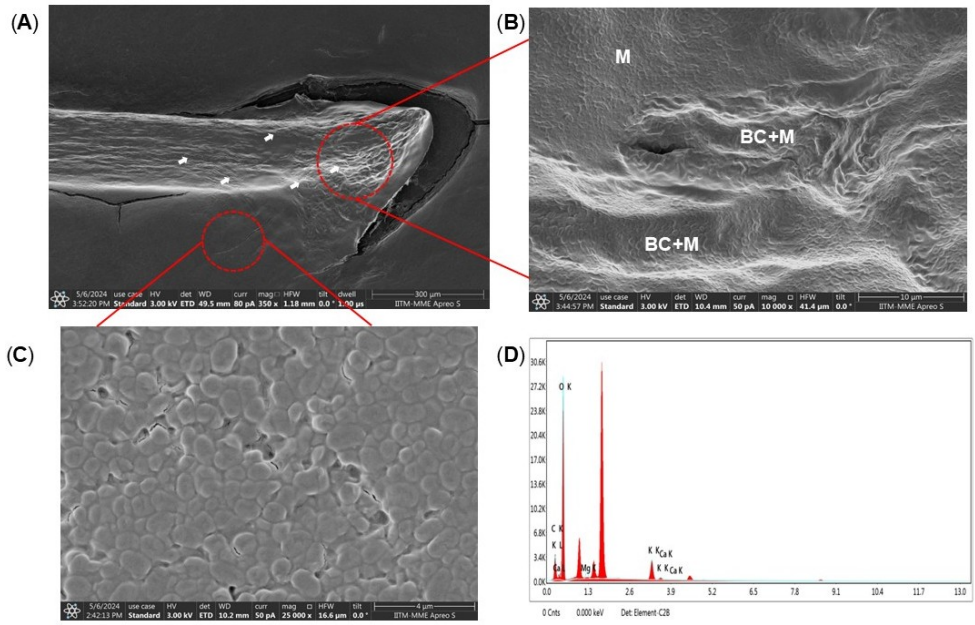

Fig. 3 Morphology of dried mung bean root mucilage obtained using Scanning Electron Microscopy (SEM). (A)Dried mucilage on the root tip. The presence of border cells is shown using white arrows. Two different regions from this image have been highlighted further (red dashed circles). (B) Root mucilage (M) along with border cells (BC). BC+M indicates regions with border cells and mucilage. (C) Mucilage morphology from a region where mucilage is free from root border cells. (D) Energy dispersive X-ray spectroscopy (EDX) analysis of dried root mucilage. EDX shows the presence of divalent (Ca^{2+}, Mg^{2+}) and monovalent (K^{+}) ions in the mucilage.

Table 1 Comparison of functional groups present in root mucilage and LM pectin from FTIR spectroscopy data

Wave number (cm^{-1})		Functional group
Mucilage	LM pectin	
3200–3500	3200–3500	stretching of hydroxyl groups
2930	2930	CH vibration of uronic acid
1600 and 1420	1600 and 1420	stretching vibration of carboxylic group of uronic acid
1000	1000	vibration of carboxylic group of uronic acid
1740	1740	ester functionality
2854	–	lipid CH_2
1642 and 1313	–	O–H bending and CH_2 symmetric bending of cellulose, respectively
1461 and 1234	–	CH- and CH_2 bond vibration of hemicellulose

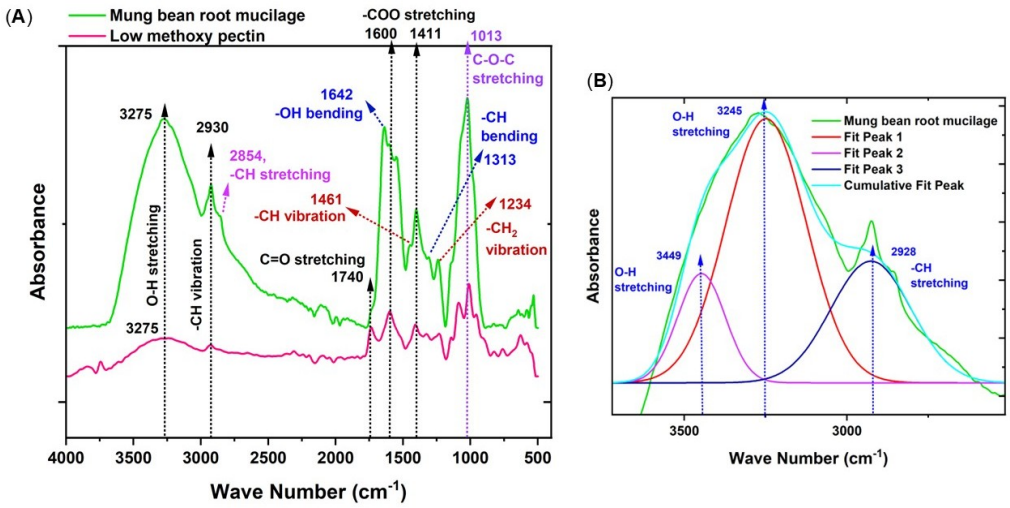

Fig. 4 Chemical structure of mung bean root mucilage using FTIR spectroscopy. (A) FTIR spectra of dry root mucilage and that of LM pectin. The dotted arrows represent the absorbance peaks corresponding to the functional groups of the polysaccharides present in the mucilage (pectin, cellulose, and hemicellulose). Free -COO group stretching at 1600 and 1411 cm^{-1}, C=O stretching at 1740 cm^{-1} and C-H stretching vibration at 2930 cm^{-1} correspond to galacturonic acid groups of the pectin present in the root mucilage and in LM pectin. The O-H bending vibration at 1642 cm^{-1} indicates the presence of cellulose, and the -CH and -CH_2 stretching vibration at 1461 and 1234 cm^{-1}, respectively, indicate the presence of hemicellulose in root mucilage. The prominent absorption peak at 1013 cm^{-1} is assigned to the symmetrical stretching vibration of the C-O-C glycosidic bond, which is characteristic of the polysaccharide structure. (B) Deconvoluted FTIR spectrum in the 3500-2900 cm^{-1} region, showing overlapping O-H stretching vibration and characteristic cellulose peaks.

To analyse the chemical composition of the mucilage, FTIR, FT-Raman, and ^{1}H-NMR studies were carried out. Seed and root mucilages are known to contain various polysaccharides, especially homogalacturonan-based pectins [54, 55]. Hence, to benchmark the physicochemical characteristics of the mucilage, low-methoxy pectin was also analysed. FTIR analysis of mung bean root mucilage is shown in Fig. 4a and summarised in Table 1. Root mucilage exhibits additional peaks at 2854, 1642, 1313, 1461, and 1234 cm^{-1}, indicating its difference in chemical composition from that of LM pectin. The characteristic broad peak observed at 3200 to 3500 cm^{-1} corresponds to the stretching of hydroxyl groups associated with the polysaccharides present in mucilage as well as the pectins. The broad peak with higher intensity present in the case of mucilage indicates additional contributions from the -OH stretching due to the

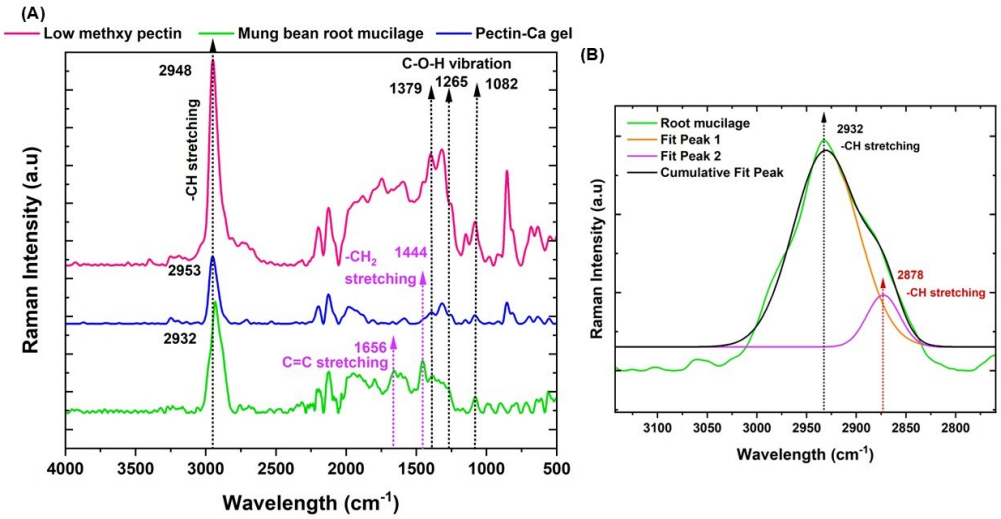

Fig. 5 (A) FT- RAMAN spectra of dried mung bean root mucilage. Spectra of LM pectin and pectin-Ca gel are also shown for comparison. The dotted arrows in the figure represent the intensity peak of functional groups corresponding to major polysaccharides. The peak in the 2930-2950 cm^{-1} region corresponds to the -CH stretching and the peaks at 1082 cm^{-1}, 1265 cm^{-1} and 1379 cm^{-1} correspond to the C-O-H vibration of the galacturonic acid group of pectins present in all three samples. (B) Deconvolution of FT-RAMAN spectra in the 2800-3000 cm^{-1} region, separates the -CH stretching of galacturonic acid of pectin from -CH and -CH_2 stretching vibrations of hemicellulose.

water present in the mucilage. LM pectin has relatively less prominent -OH stretching. The peak in the 2930 cm^{-1} region indicates -CH vibration and peaks at 1600 cm^{-1} and 1411 cm^{-1} indicate the stretching vibration of the carboxylic group of uronic acid which originates from the pectin polysaccharides. The band in the 1013 cm^{-1} region can be assigned to –C-O stretching of carbohydrates. The peak observed at 1740 cm^{-1} in LM pectin and the mucilage corresponds to the ester functionality. This peak merges with the peak at 1640 cm^{-1} in the case of the root mucilage and is visible as a shoulder. The peak at 2854 cm^{-1} indicates the symmetric stretching of lipid CH_2 [56]. The additional peaks at 1642 cm^{-1} and 1313 cm^{-1} indicate the O-H bending of cellulose [57] and CH_2 symmetric bending of cellulose [58] respectively. The peaks at 1461 cm^{-1} and 1234 cm^{-1} are due to CH- and CH_2 bond vibration of hemicellulose [59]. To better understand the peaks around 3200-3500 cm^{-1}, the spectra were deconvoluted

and are shown in Fig. 4B. The peaks at 3449 cm^{-1}, 3245 cm^{-1} and 2928 cm^{-1} correspond to O-H stretching, H-bonded O-H stretching and C-H stretching respectively and indicates the presence of cellulose in the mucilage [60–62].

The FT-Raman spectra of the dried root mucilage, LM pectin, and pectin-Ca gel for comparison are shown in Fig. 5A. The peak at 2930-2950 cm^{-1} region corresponds to symmetric and asymmetric -CH stretching of pectin [63]. However, deconvolution of the spectra (Fig. 5B) also shows a peak at 2878 cm^{-1} corresponding to the hemicellulose present in the mucilage [64]. The peaks in the 1400-1460 cm^{-1} region correspond to the stretching of -CH_2 bonds of sugars such as xylose, arabinose, and the CH_3 group of rhamnose [65]. The peaks at 1082 cm^{-1}, 1265 cm^{-1} and 1379 cm^{-1}, are assigned to the C-O-H vibration modes of galacturonic acid [65]. These can be observed in the case of LM pectin as well as in the root mucilage. Peaks observed at 1656 cm^{-1} and 1444 cm^{-1} indicate the presence of phospholipid [66]. In the case of LM pectin, free carboxyl groups (-COO-) exhibit distinct and strong vibrational mode peaks at 2948 cm^{-1}. The intensity and the position of this peak change during crosslinking of the carboxyl groups, as can be observed in the case of pectin-Ca gel and the mucilage.

^{1}H-NMR study was also carried out on the mucilage and is given in Supplemental Fig. **S1**. The crowded and narrow region between 3 to 5 ppm in the ^{1}H NMR spectra, characteristic of polysaccharides, indicates the presence of numerous sugar residues [67]. The signals between 3.1 to 4.3 ppm are due to non-anomeric protons (H_2-H_6) and the signals between 4.3 to 4.8 ppm arise from α-anomeric protons [68]. The regions associated with α-anomeric carbons suggest the presence of several sugar residues, including arabinose, galactose, rhamnose, and xylose as the neutral sugars [69]. The peaks at 3.93 ppm, 3.91 ppm, 3.58 ppm, 3.63 ppm, and around 2.28 ppm confirm the xylose, arabinose, OH, and CH groups of mannose, rhamnose, and uronic acid, respectively [70], indicating the presence of pectin polysaccharides in the root mucilage.

Previous studies on cress, maize, and rice reported the presence of uronic acid along with arabinose, galactose, rhamnose, and xylose in their root mucilage [71].

To confirm the monosaccharide composition inferred from the ^{1}H-NMR spectra, HPLC analysis of acid-hydrolysed root mucilage, along with standard monosaccharides (four sugars-xylose, arabinose, galactose, and rhamnose), was carried out and is given in Supplemental Fig. **S2**. From individual runs, the retention times for these sugars are - 10.838 min (galactose), 10.857 min (xylose), 11.425 min (rhamnose), and 11.776 min (arabinose). From the mixture run, three distinct peaks appear with retention times of 10.858, 11.441, and 11.748 min, indicating the overlapping galactose and xylose peaks as a broad peak at 10.858 min since their retention times are very close to each other. The chromatogram of root mucilage indicates two distinct peaks with retention times at 10.786 and 11.748 min. This could be due to the overlapping of peaks with a small difference in retention time. Galactose and xylose appear as an overlapped peak at 10.786 min, whereas rhamnose and arabinose appear as an overlapped peak at 11.748 min.

4.3 Drying, re-hydration ability and soil wetting characteristics

Drying and re-hydration dynamics of the root tip with mucilage were studied using a tensiometer setup by placing the root tip from its needle and observing the diameter changes using the goniometer camera. The experiment was carried out at 25 °C and 60% RH as mung bean is reported to grow well at low soil humidity (60% RH) [72]. The images obtained at different time intervals are shown in Fig. 6. Changes in the diameter of the mucilage drop (D_M)(taken at the mid-point of the mucilage drop as shown in Fig. 6) and the root tip (D_R) were determined from a series of images taken, capturing the progressive stages of drying and subsequent re-hydration followed by a second drying step (shown in Fig. 7). During the first drying phase, the root diameter remained constant for a considerable duration (up to 80 min), showing no changes until

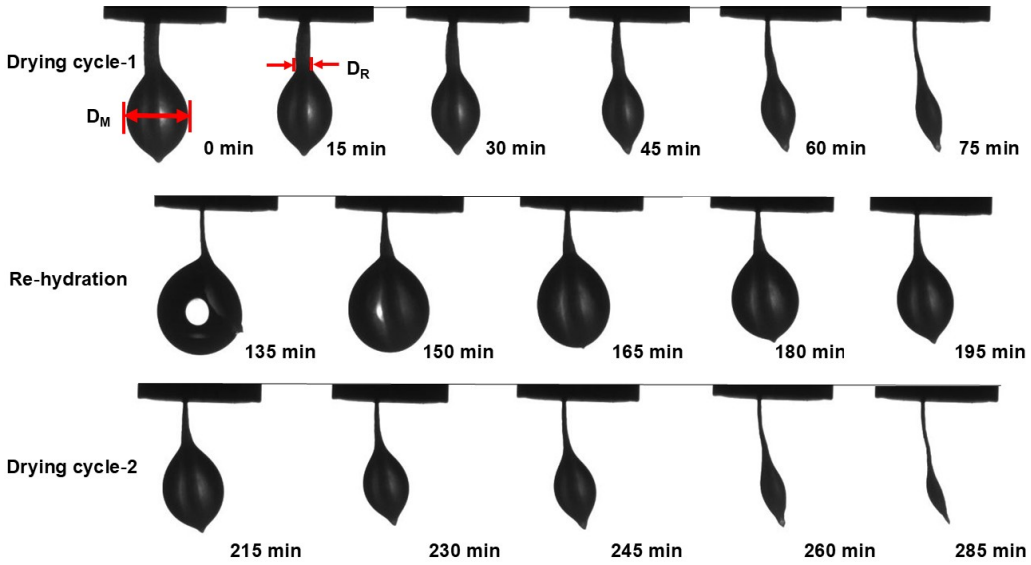

Fig. 6 Optical images of the root tip with mucilage during drying-rehydration cycles. 3-day-old mung bean root tip with exuded mucilage was subjected to drying in air at 25 °C and 60% RH (Drying cycle-1). Optical images were obtained using the goniometer camera. Mucilage diameter (D_M) and root diameter (D_R) are estimated from the collected images using the ImageJ software. As the water evaporates, the volume and diameter of the mucilage drop on the root tip decrease and form a very thin layer with no further change in the diameter of the mucilage and the root tip (equilibrium drying) by the end of drying cycle-1. At this stage, a known volume of deionised water (0.5 μL) was introduced at the root tip, and the dried mucilage starts to swell slowly by imbibing water (Re-hydration phase) until the root and mucilage drop diameter reaches the equilibrium swelling (original D_M and D_R values before starting the drying cycle-1). The same swollen mucilage drop was again allowed to dry for a second time (Drying cycle-2), which followed a similar trend to that of drying cycle-1. A quantitative representation of these drying and re-hydration dynamics of the root and root with the mucilage is shown in Fig. 7. Images in Fig. 6 are representative only and not exactly corresponding to the values shown in Fig. 7. Experiments were repeated multiple times to obtain reliable data.

the mucilage layer dries to a significant extent (mucilage diameter decreased from 0.74 mm to 0.2 mm). The root diameter started to decrease from the initial 0.13 mm after 80 min drying. At 120 min, both the mucilage and root diameter reduced considerably and became constant (0.02 mm). After a gap of 15 min, water was introduced to re-hydrate the mucilage. The diameter of both the mucilage and the root started to increase. However, the root attained the original diameter of 0.13 mm much faster (in 20 min) than the mucilage, which took a longer time (60 min) to reach the original swollen drop diameter. A notable observation is a slight delay in the re-swelling of the root, which follows a non-linear path to reach the original diameter. Once the mucilage diameter

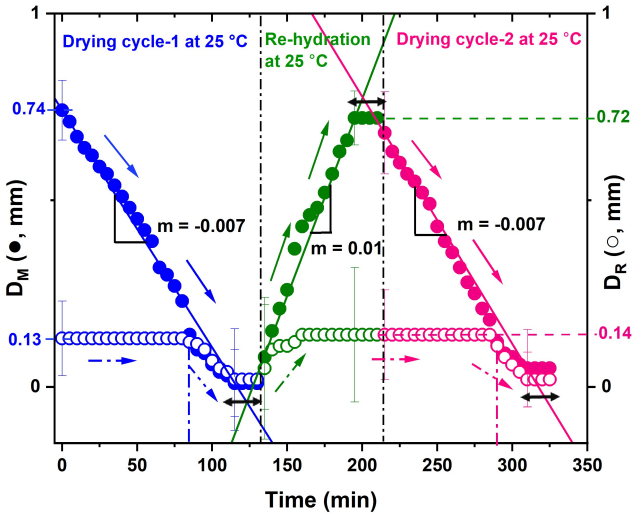

Fig. 7 Role of mucilage in protecting the root tip from drying up. Variation of mucilage diameter (D_M, filled circles) and root diameter (D_R, empty circles) as a function of drying time is shown. First cycle of drying was followed by a re-hydration cycle and a second cycle of drying of the same root tip with mucilage. This was carried out at 25 °C and 60% RH. The slope (m) of the diameter variation is obtained by fitting the experimental data points to a linear regression fit. Blue, green, and pink symbols correspond to drying cycle-1, re-hydration, and drying cycle-2, respectively. Solid and dashed single-headed arrows indicate the continuous direction of drying and re-hydration cycles. Double-headed black arrows represent the equilibrium dried/swollen state of the root and the mucilage. The values 0.13 and 0.14 on the Y-axis represent root diameter, which remains constant for a significant extent of the drying period. Data points are representative values from three sets of experiments repeated on different root tips.

exceeded 0.2 mm, the root diameter did not change further, indicating an equilibrium re-swelling state. From 195 to 215 min there was no change in mucilage diameter due to the mucilage being at the equilibrium swelling. After remaining unchanged for 15 min, the diameter started to decrease. A similar drying dynamics comparable to that of the first drying phase could be observed. The root diameter remained unchanged initially until the mucilage layer started to shrink. When the mucilage diameter reached < 0.2 mm, the root diameter also began to decrease, eventually reaching a constant value of 0.14 at 310 min. This indicates the protective nature of the mucilage present at the root tip for a significant duration before it starts affecting the root. Tracking the thickness of the mucilage layer during drying provides insights into the response of the root to moisture loss, showing shrinkage patterns and structural changes. When water was

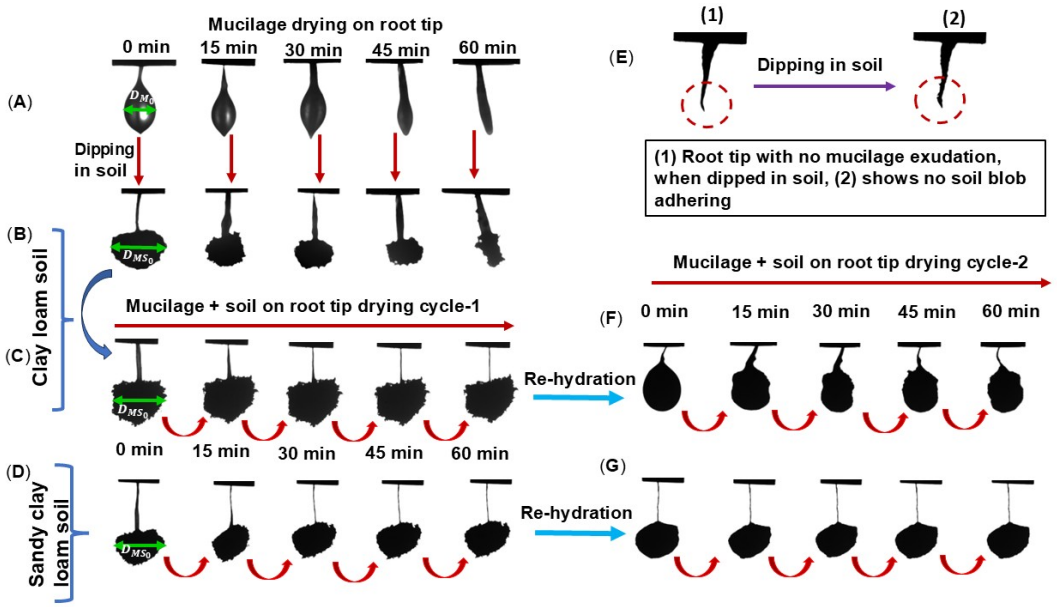

Fig. 8 Root-soil interactions and wetting of the soil by the freshly exuded mucilage present on the root tip. Drying and rehydration effects of the mucilage on root-soil interactions were obtained from the optical images collected using a Goniometer camera. The obtained images were analysed using ImageJ software to estimate D_{M_0}, D_{MS_0} as a function of time. Row (A) shows five different root tips with mucilage dried for 0 min, 15 min, 30 min, 45 min, and 60 min durations. These root tips were dipped in clay loam soil and are shown in Row (B). Root tips dried for longer durations show less amount of soil adhering to the root tip. To test the effect of continuous drying on the root-mucilage-soil stability, first blobs shown in Rows (C) and (D) were allowed to dry for 60 min durations. Row (D) shows drying of the root tip with mucilage dipped in sandy loam soil. The blob diameter is monitored as a function of drying time (D_{MS_t}). Row (E) shows how the root tip with no mucilage has very little soil adhering to it. Rows (F) and (G) show the re-hydration behaviour of root tips with mucilage and soil blobs after 60 min drying periods. Normalized diameter, D1 ($\frac{D_{M_t}}{D_{M_0}}$) and D2 ($\frac{D_{MS_t}}{D_{MS_0}}$) used in Fig. 9 were estimated from these measurements. Representative image from three independent experiments is shown.

reintroduced to the dried root tip, the mucilage starts to re-hydrate, allowing quick and effective absorption of water, returning the root to its hydrated state. Drying and re-hydration dynamics of the root tip with mucilage were studied using a tensiometer setup by placing the root tip from its needle and observing the diameter changes using the goniometer camera. The experiment was carried out at 25 °C and 60% relative humidity (RH) as mung bean is reported to grow well at low soil humidity (60% RH) [72]. The images obtained at different time intervals are shown in Fig. 6. Changes

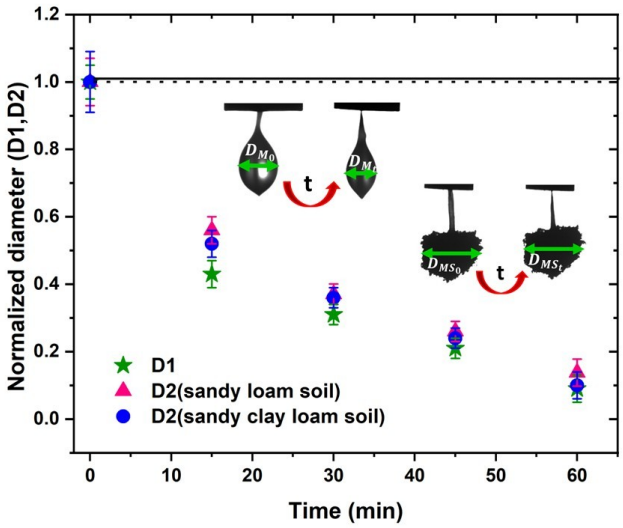

Fig. 9 Effect of mucilage layer on the root tip during the drying of soil. Data from Fig. 8 is used for estimating the normalized diameters, D1 ($\frac{D_{M_t}}{D_{M_0}}$) and D2 ($\frac{D_{MS_t}}{D_{MS_0}}$). The black dashed line represents the diameter of the root with no mucilage exudation. The back solid lines represent the diameter of the root after dipping into the soil when there is no mucilage exudation from the root tip. Root tips with mucilage show a decrease in the soil blob diameter as a function of drying time. Sandy clay loam soil shows higher shrinkage or drying in comparison to sandy loam soil. Mung bean is shown to grow better in sandy loam soils. D_{M_0}, diameter of the root+mucilage at time t=0; D_{M_t}, diameter of the root+mucilage drop at time t ; D_{MS_0}, diameter of the root+mucilage+soil blob at time t=0; D_{MS_t}, diameter of the root+mucilage+soil blob at time t. Reported values are the average (±SD) from three independent experiments.

in the diameter of the mucilage drop (taken at the mid-point shown in figure) and the root tip were determined from a series of images taken, capturing the progressive stages of drying and subsequent re-hydration followed by a second drying step (shown in Fig. 7). During the first drying phase, the root diameter remained constant for a considerable duration (up to 80 min), showing no changes until the mucilage layer dries to a significant extent (mucilage diameter decreased from 0.74 mm to 0.2 mm). The root diameter started to decrease from the initial 0.13 mm after 80 min drying. At 120 min, both the mucilage and root diameter reduced considerably and became constant (0.02 mm). After a gap of 15 min, water was introduced to re-hydrate the mucilage. The diameter of both the mucilage and the root started to increase. However, the root attained the original diameter of 0.13 mm much faster (in 20 min) than the mucilage,

which took a longer time (60 min) to reach the original swollen drop diameter. A notable observation is a slight delay in the re-swelling of the root, which follows a non-linear path to reach the original diameter. Once the mucilage diameter exceeded 0.2 mm, the root diameter did not change further, indicating an equilibrium re-swelling state. From 195 to 215 min there was no change in mucilage diameter due to the mucilage being at the equilibrium swelling. After remaining unchanged for 15 min, the diameter started decreasing. A similar drying dynamics comparable to that of the first drying phase could be observed. The root diameter remained unchanged initially until the mucilage layer started to shrink. When the mucilage diameter became < 0.2 mm, the root diameter also began to decrease, eventually reaching a constant value of 0.14 at 310 min. This indicates the protective nature of the mucilage for a significant duration before it starts affecting the root. Tracking the thickness of the mucilage layer during drying provides insights into the response of the root to moisture loss, showing shrinkage patterns and structural changes. When water was reintroduced, the re-hydration of the mucilage was observed, allowing measurement of how quickly and effectively it could absorb moisture and return to its hydrated state.

A series of novel experiments were designed to investigate the root-soil interactions using freshly exuded root mucilage present on the root tips, as shown in Figure 8. Mung bean root tips with fresh mucilage dipped in soil and taken out were subjected to drying and re-wetting. The diameter of the soil blob at the mid-point (D_{MS}) obtained using optical image analysis (ImageJ software) was used to correlate with the amount of soil adhering to the root tip. Row A, in Figure 8, shows 5 different root tips dried for different durations of time. At 0 min, the mucilage appears to cover the root tip fully. On root tip 2 (dried for 15 min), a slight reduction in diameter can be observed as a result of mucilage drying. On root tip 3 (dried for 30 min), the mucilage layer becomes noticeably thinner. On root tips dried for 45 and 60 min, the mucilage layer is significantly depleted. These root tips with mucilage dried to different extents were

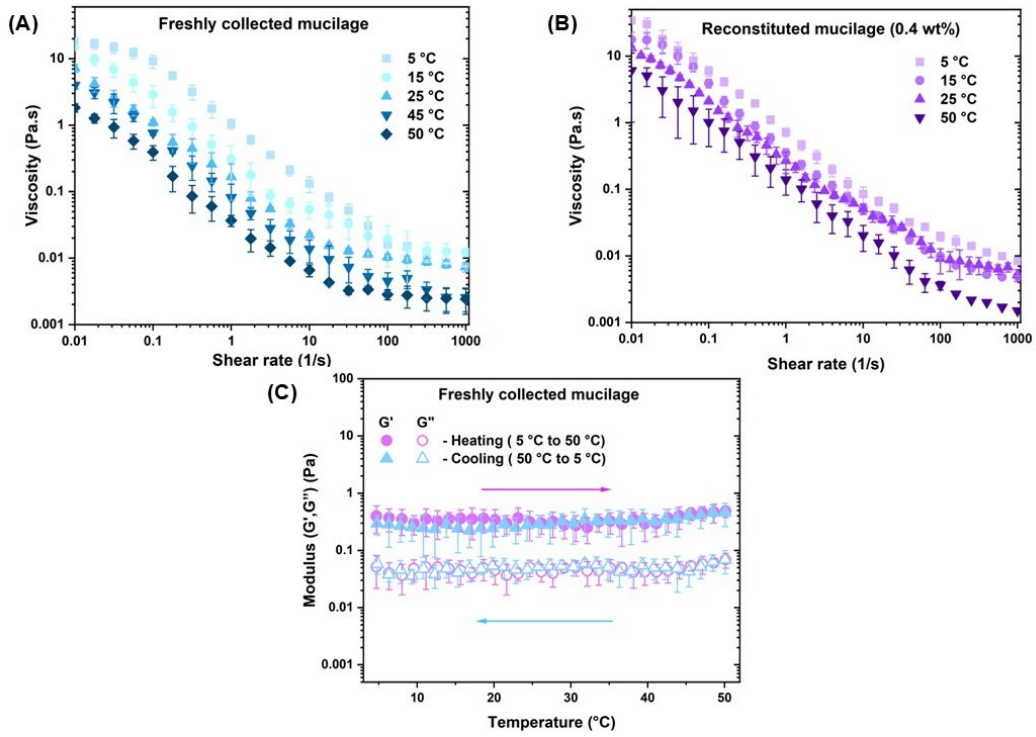

Fig. 10 Temperature sensitivity of mung bean root mucilage: Effect of temperature and shear rate on the viscosity of (A) fresh mung bean root mucilage and (B) reconstituted mung bean root mucilage. (C) storage (G') and loss (G") modulus variation of fresh mung bean root mucilage to heating (5 to 50 °C) and cooling (50 to 5 °C) cycles show the thermo-reversible nature of the mucilage (at 1% strain and frequency-1 rad/s). Viscosity and modulus data reported are the average (±SD) of five independent samples from five different batches.

dipped in clay loam soil, and the corresponding images are shown in row B. These images show a clear relationship between the quantity of mucilage and the amount of soil adhering to the root tip. The root tip with no drying holds the largest soil blob. This indicates the wetting capability of the freshly exuded mucilage and the water availability. Root tip with mucilage dried for 15 min show a clear reduction in the amount of soil adhering to it. Root tips dried for 45 and 60 min show very small quantities of soil adhering to them. These results show that the capacity of the mucilage to spread and wet the soil decreases with increasing durations of the drying period. Row C has a root tip holding fresh mucilage (0 min drying) and clay loam

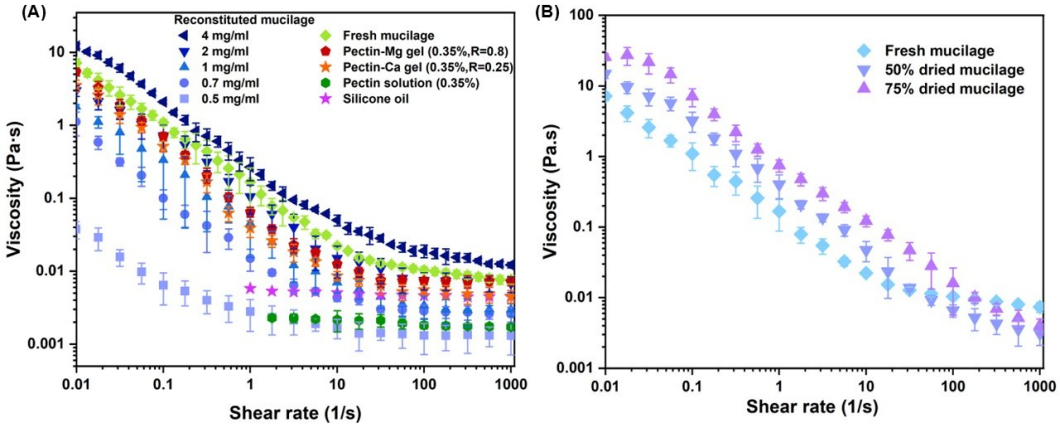

Fig. 11 Shear-dependent viscosity of freshly collected mung bean root mucilage. (A) Steady shear response showing the shear thinning behaviour of the fresh root mucilage and the reconstituted mucilage. Pectin gels (Ca and Mg-crosslinked) and reconstituted root mucilage show shear thinning followed by a Newtonian plateau at higher shear rates. Pectin solution of comparable concentration to that of mucilage (0.35 wt%) and silicone oil show Newtonian fluid-like response throughout the shear rate range. This shows how crosslinking by Ca and Mg ions changes the response of the mucilage and the role of pectin polysaccharides. (B) Viscosity of the fresh mucilage increases significantly as the water content decreases due to drying. Viscosity data is the average (±SD) obtained from five independent experiments.

soil blob adhering to it. This root tip with soil blob is allowed to dry in the air for 60 min before subjecting it to re-hydration (row F). During the drying process of the soil blobs adhering to the root tip, it may be noticed that only slight changes in the size and structure of the soil blob were observed. This is in contrast to that of the drying behaviour of the mucilage drop without the soil present on the root tip. Following the drying cycle, the soil blob was re-hydrated. This leads to a slight increase in the soil blob size. Drying and re-hydration experiments were also conducted using sandy clay loam soil, and the results are shown in rows D and G, respectively. It can be observed from the images shown in rows C, D, F and G that the behaviour of both the soil types is comparable during drying and re-hydration. In row E, a root tip with no mucilage (less humid air) shows very little soil adhering to the root tip. This indicates the significant role of the wet mucilage in spreading into the soil around the growing root tip and in holding it together in the rhizosphere. These experimental observations are

summarised in Fig. 9. In the presence of mucilage, both sandy loam and sandy clay loam soils adhered to the root tip, forming a distinct soil blob around it. Observations show that mucilage facilitated the aggregation of soil particles into a cohesive mass surrounding the root surface and stayed on the root tip for a significant amount of time. To analyse this behaviour quantitatively, the ratio of the diameter of the soil blob at different times to the initial diameter of the blob ($\frac{D_{MS_t}}{D_{MS_0}}$) was estimated over time for each type of soil. The dashed and solid lines represent the root, which did not produce any mucilage (grown under non-humid conditions), and exposure to soil led to very few soil particles adhering to the root tip. The drying and re-hydration behaviour of the root mucilage was also studied by observing the changes in the root tip kept on a glass slide using an optical microscope (Supplemental Fig. **S3**). In row A, it can be observed that the root diameter does not change when the mucilage layer is present on the root tip. However, when the thickness of the mucilage layer decreases significantly due to drying (60 min), the root diameter gets affected. Upon rehydration (row B images), the root as well as the mucilage layer starts to re-swell and reach the dimensions as before. These observations support the role of mucilage in protecting the root tip against excessive dehydration up to a certain time.

4.4 Temperature sensitivity of the root mucilage

Rheological response of hydrogels at different temperatures and for varying shear rates is known to originate from the gel network structure of the polymers involved, as well as the type of crosslinks. Since root mucilage shows weak gel-like behaviour, it is further investigated using rheology to understand how its structure would contribute to its mechanical response and thus to the environmental conditions. Soil temperature can vary significantly due to factors such as time of day, season, and depth of the soil. In this context, we investigate the temperature sensitivity of the mucilage relevant to the soil temperature fluctuation range (5 to 50 °C). These temperatures were chosen to

represent the possible soil temperatures [73]. Fig. 10A shows the variation of viscosity of the fresh mung bean root mucilage at different temperatures. For comparison, the viscosity variation for reconstituted mung bean root mucilage at different temperatures is also shown in Fig. 10B. The apparent viscosity shows a decrease with increasing temperature. The low and high shear Newtonian plateau visible in the amplitude sweep results at lower temperature (5 °C) changes into more shear thinning behaviour at higher temperatures, and the higher shear rate Newtonian Plateau extends further at higher temperatures. This indicates the mucilage becomes more fluid-like at higher temperatures, and the viscosity drops by one order of magnitude. The interactions between the polymer chains in the mucilage, such as the hydrogen bonds and the electrostatic interactions, get disrupted as the thermal energy causes the chains to undergo conformational changes at higher temperatures. A Newtonian plateau is observed at higher shear rate after shear thinning, whereas at 5 °C, the Newtonian plateau is not significant, indicating that the mucilage maintains gel-like nature at lower temperatures. To examine the temperature sensitivity, the fresh mucilage was subjected to a heating and cooling cycle between 5 and 50 °C. The variation of the elastic and the loss moduli as a function of temperature is shown in Fig. 10C. The results indicate that the mucilage consistently retains its gel-like structure by maintaining an elastic-dominated behaviour (where $G'>G''$). The violet arrow represents the response to the heating from 5 to 50 °C and the blue arrow represents the response to the cooling from 50 to 5 °C. Up to 40 °C, both G' and G" remain constant. However, above 40 °C, there is a very small increase in the modulus values indicating minor structural changes. However, due to the reversible nature of this behaviour while undergoing cooling, this can be considered as arising from H-bond re-organisation, which is reversible.

4.5 Role of mucilage in reducing shear forces during root growth

The effect of temperature, a key soil condition, on mucilage behaviour was discussed in the previous section. During growth, plant roots also experience various shear forces depending on the type of soil, soil porosity, water content, etc.. Root mucilage is known to enable the penetration of the root tip into the soil. Steady shear rheological measurements of gels and fluids under varying shear rates are used to understand and mimic the shear conditions experienced under various application conditions and in biological conditions. Unique rheological responses of fluids also originate from their chemical and molecular structure. Hence, to understand the mechanical response of the mucilage during root growth and root penetration through the narrow soil pores, steady shear rheological studies on the fresh mung bean mucilage were carried out. The contributions from the chemical and molecular structure of the root mucilage is used for interpreting the shear response.

4.5.1 Rheological behaviour

Temperature, which is one of the important soil conditions, can affect the behaviour of mucilage and has been discussed. Viscosity variation of fresh mung bean root mucilage with shear rate is shown in Fig. 11A. Viscosity variation of the reconstituted root mucilage at different concentrations, pectin solution, and gels of pectin-Ca and pectin-Mg are also shown for comparison. Comparison of fresh and reconstituted root mucilage behaviour with pectin solution (0.35 wt% solid content) shows that crosslinking is important to form the gel structure both in mucilage and pectin. The pectin concentrations and crosslink ratios were selected based on the solid content of the mucilage. Ca and Mg crosslinking result in slightly different shear responses, with Mg requiring higher concentrations to reach a similar viscosity as that of the

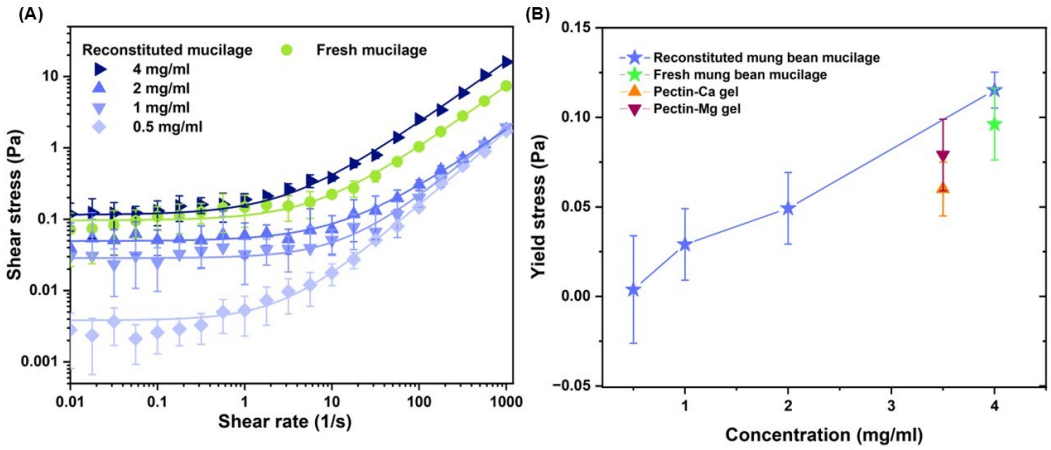

Fig. 12 Yield stress behaviour of fresh mung bean root mucilage. (A) Shear stress variation as a function of shear rate for fresh and reconstituted mucilage is shown. The data is fitted using a simplified Herschel-Bulkley model (Equation 3). The yield stress values obtained from this fit (Table S1, supplemental data) are shown in (B) as a function of concentration for the reconstituted mucilage. The value of yield stress for reconstituted root mucilage shows a gradual increase with an increase in concentration. For fresh mucilage and pectin gels, the single data point given is the average of multiple measurements carried out on different samples, and it corresponds to a particular concentration indicative of the solid content of freshly collected mucilage. The data shown is the average (±SD) of five independent experiments.

fresh mucilage. This indicates that the gel structure of the root mucilage is predominantly Ca-ion-based. The viscosity of freshly collected mucilage and reconstituted root mucilage decreases with increasing shear rate and reaches a Newtonian plateau (infinite shear viscosity, η_∞) at higher shear rates. Steady shear experiments on standard Newtonian fluid (silicone oil) are also shown in the same figure to highlight the shear-thinning nature of all the other systems studied (uncrosslinked pectin solution also shows a Newtonian behaviour). The viscosity increases with solid content in the case of reconstituted mucilage. Compared with the reconstituted mucilage of varying concentrations, the zero shear viscosity of the fresh mucilage is equivalent to the viscosity of reconstituted mucilage with a solid content between 2-4 mg/ml. The decrease in viscosity with increasing shear rate indicates shear-thinning behaviour of the mucilage. This behaviour is commonly seen in hydrogel and hydrocolloid systems due to their large molecular size and polymeric network structure, due to ionic crosslinks as well

as H-bonding [74, 75]. However, at higher shear rates, the mucilage behaves more like a Newtonian fluid (plateau region).

Another question is to understand how the mucilage responds to drying. The effect of drying (or water loss) on the viscosity of fresh root mucilage is shown in Fig. 11B. In the case of freshly collected root mucilage, the high shear rate plateau region vanishes with drying. This indicates that the contributions from the pectin polysaccharide dominate even at high shear rate, as water evaporates from the gel.

Shear response of several biomedical gels [76], lubricants [77], foods and cosmetics [78] have been described using the Herschel-Bulkley (H-B) model. This model provides a relation between shear stress (τ) and shear rate ($\dot{\gamma}$) as follows:

$$\tau = \tau_0 + k\dot{\gamma}^n \tag{3}$$

where k is the consistency coefficient (Pa.s^n), τ_0 is the yield stress (Pa), and n is the flow behaviour index. Figure **12A** shows that the H-B model can be used for fitting the experimental $\dot{\gamma}$ vs τ results to describe the flow behaviour of the mucilage. At high shear rates, the mucilage exhibits a $\dot{\gamma}$–τ relationship of a strongly shear-thinning fluid. However, at low shear rates, the shear stress reaches a plateau value indicative of yield stress behaviour. Below this yield stress (< 0.1 Pa.s), the mucilage behaves like a viscoelastic solid-like material, which can maintain its shape and structure. This could also be the reason why the mucilage with a definite shape could be observed to form at the root tip under a humid air environment (Subsection-Drying, re-hydration ability and soil wetting characteristics). In the case of reconstituted mucilage, with increasing concentration. There is a corresponding increase in the yield stress values (Fig. 12B). The values of k and n from the H-B model fit are shown in Supplemental Table S1. There is an increase in k with an increase in the concentration, indicating that the gel has higher viscosity due to a greater number of polymer chain interactions

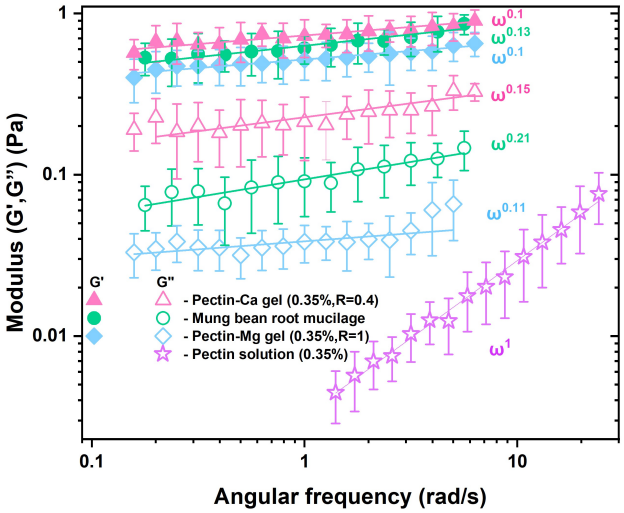

Fig. 13 Gel-like behaviour of fresh mung bean root mucilage obtained from the frequency sweep data. Frequency-dependent behaviour (Equation 4) of storage (G') and loss (G'') modulus at 1% strain amplitude and 25 °C of root mucilage and pectin gels shows a viscoelastic, weak gel-like response (b∼0.1-0.2). Pectin solution (un-cross-linked) shows viscous fluid-like behaviour (b=1). The data shown is the average (±SD) of five independent experiments.

and network formations. Correspondingly, n decreases with increasing concentration, indicating that the gel becomes more shear-thinning. At higher concentrations, the polymer network resists flow at low shear rates. However, at higher shear rates, the network breaks down to a greater extent, causing a significant decrease in viscosity.

The change in modulus as a function of frequency (ω) is expressed as

$$G'(\omega),\, G''(\omega) \propto \omega^{b} \tag{4}$$

The variation of modulus for fresh and reconstituted mucilage is shown in Fig. 13. The pectin solution exhibits a purely viscous nature, with the loss modulus (G") higher than the storage modulus (G') and following a power-law factor of b=1, indicative of its fluid-like behaviour. In contrast, the root mucilage and pectin-Ca/Mg gels consistently show higher G' than G" across the entire frequency range, with no crossover observed, signifying their viscoelastic gel-like behaviour with elasticity dominating. A Power-law

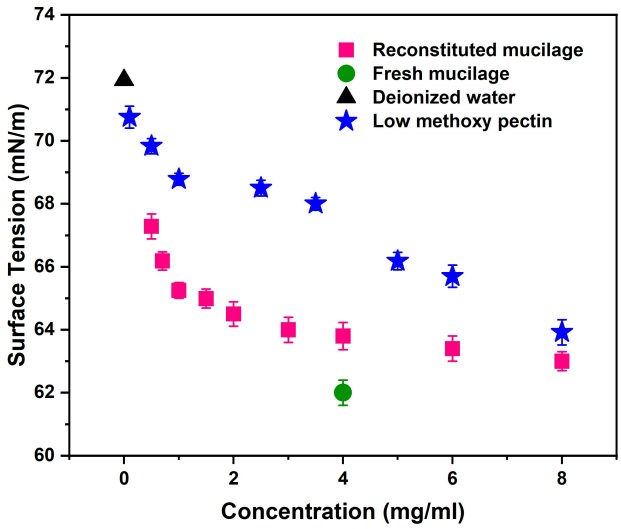

Fig. 14 Surface tension of fresh mung bean root mucilage obtained from pendant drop experiments. The effect of concentration variation on the surface tension of reconstituted root mucilage and LM pectin solutions in comparison to deionised water is also shown (at 25 °C). Both LM pectin and reconstituted root mucilage show a decrease in surface tension with increasing concentration. For fresh mucilage, the single data point (green symbol) is the average of multiple measurements carried out on the fresh mucilage collected from different batches of seedlings grown. The data shown is the average (±SD) obtained from five independent experiments.

model could fit both G' and G'' with b ranging from 0.1 to 0.2. These exponents, being much lower than 1, indicate a weak frequency dependence of the moduli, indicating a well-defined, stable network structure. The deviation from a factor of 1 highlights the transition from a purely viscous behaviour (as seen in the pectin solution) to a viscoelastic gel-like state. This weak scaling suggests that the storage modulus (G') and loss modulus (G'') increase only slightly with frequency, further underscoring the dominance of the elastic nature of the gels over their viscous behaviour.

4.5.2 Wetting behaviour in the soil

Figure 14 shows the surface tension of the freshly collected mung bean root mucilage. Surface tension values for the reconstituted root mucilage at different concentrations and those of low methoxy pectin solutions are also shown for comparison with fresh

mucilage. Surface tension value of fresh mucilage is obtained as the average of multiple measurements carried out on fresh mucilage collected from different seedlings grown in different batches. The surface tension of fresh mung bean root mucilage is 62 mN/m. Reconstituted mucilage solutions in water show higher surface tension than fresh mucilage and decrease with increasing concentration. When compared with the surface tension of deionised water (∼72 mN/m), fresh mucilage shows a considerable decrease in surface tension. Pectin solutions in water also show a decrease in surface tension with increasing pectin content, but not comparable to that of the mucilage. Pectin requires much higher concentrations to obtain a comparable reduction in surface tension as that of the fresh mucilage. In addition to the xylose, rhamnose, and galactose present in the mucilage, the phospholipids, which are amphiphilic molecules, may be contributing to the lowering of the surface tension in fresh mucilage. The slightly higher surface tension in reconstituted mucilage could be due to the changes in H-bonds due to processing.

The role of surface tension and viscosity of the mucilage can be further analysed using the Ohnesorge number (Oh), a dimensionless number that describes the effect of both viscous and surface tension forces on the mucilage flow and wetting, including its behaviour within a porous medium, such as soil.

$$\mathrm{Oh} = \frac{\eta}{\sqrt{\rho\,\sigma\,r}} \tag{5}$$

where η is the mucilage viscosity [Pa.s], σ is the mucilage surface tension [N/m], ρ is the mucilage density [kg/m^3], and r is the characteristic length (m). 'r' is used in two different contexts: as drop diameter (D_M = r) for estimating Oh for fresh mucilage drop. In the case of root-soil interaction through mucilage, the soil pore size is used as the characteristic length (r). Using the experimentally determined values of viscosity (η = 0.16 Pa.s at the shear rate of 1 s^{-1} as mucilage is a yield stress fluid), surface

tension ($\sigma = 62$ mN/m), and density ($\rho = 1050$ kg/m^3) for freshly collected mucilage, and considering the mucilage drop diameter (D_M=0.75 mm), Oh is obtained as 0.7 (Oh < 1). A higher Oh number (Oh > 1) indicates viscous forces are dominant over surface tension forces. Whereas, a low Oh number (Oh < 1) signifies that surface tension primarily governs the mucilage behaviour and controls the spreading of the mucilage. In the second case of root soil interaction, we used the soil pore size as the characteristic length (r) to estimate the Oh number. The average pore size of the sandy clay loam and sandy loam soil was used for the Oh number estimation and summarized in Table 2. The Ohnesorge number is lower for sandy loam soil, indicating its better suitability for mucilage spreading in the soil.

Table 2 Ohnesorge number (Oh) estimated for mucilage in sandy loam and sandy clay loam soil

Soil type	**Soil Pore Diameter (µm)**	**Ohnesorge Number**
Sandy clay loam	lowest -50	2.8
	highest - 100	1.9
Sandy loam	lowest -100	1.9
	highest -300	1.1

The contact angle of root mucilage in comparison to water on different substrates is shown in the Supplemental Fig. **S4** and **S5**. On a glass substrate, water exhibits a low contact angle of 18°, indicating excellent wetting, while root mucilage shows a higher contact angle of 45°, suggesting moderate wetting. This indicates that mucilage, while capable of interacting with hydrophilic surfaces, does not spread as readily as water, possibly due to its higher viscosity or complex molecular structure. However, on the Teflon substrate, water shows a high contact angle of 102°, reflecting poor

wetting, whereas root mucilage has a slightly lower contact angle of 94°, indicating better wetting than water on hydrophobic surfaces. These indicate that mucilage may contain hydrophilic and hydrophobic domains.

5 Discussion

Various spectroscopic and HPLC data analysis suggest the presence of distinct pectic polysaccharides (pectins) in mung bean root mucilage. FTIR spectra show strong bands associated with galacturonic acid present in the homogalacturonan (HG) backbones that form the principal linear domains of pectin. These HG domains of the pectin molecules, with low methyl esterification (shown by the weak ester carbonyl band at 1740 cm^{-1} can interact with the divalent cations, Ca^{2+} and Mg^{2+} and form ionically cross-linked gel structure in the root mucilage. Results obtained from the FTIR analysis indicate the presence of low-methoxy pectin as the dominant component in fresh mung bean root mucilage, evidenced by absorption peaks at 1600 cm^{-1} and 1740 cm^{-1}. ^{1}H-NMR and HPLC analysis of the mucilage show the presence of monosaccharides, dominated by pentoses such as rhamnose, arabinose, xylose and hexose such as galactose, which are typical components of rhamnogalacturonan I (RG-I). This distinguishes mung bean root mucilage significantly from that of maize root mucilage, which is shown to be hexose-rich [79]. *Bradyrhizobium*, a nitrogen-fixing bacteria, has been shown to be the only rhizobial inhabitant of mung bean nodules in tropical soils [80]. The *Bradyrhizobium genus* is metabolically optimised to utilise pentose sugars as its preferred carbon and energy sources [81, 82]. Hence the findings that the mung bean root mucilage is rich in pentose sugars favoured by the Bradyrhizobium points to the relationship between the Nitrogen fixing bacteria present in the root nodules of mung bean and its root mucilage. In maize, however, only one known species, Sierra Mixe maize, has been reported to obtain nitrogen through an association with nitrogen-fixing microbes present in its aerial root mucilage via diazotrophic [83]. The

composition of maize aerial root mucilage is rich in hexose sugars, unlike the mung bean root mucilage. The selectivity for specific sugars by the nitrogen-fixing bacteria found in these two species thus differs. The gel formation ability of HG and RG-I galacturonans is well understood from various studies. By combining this gel-like mucilage with bacterial extracellular polymeric substances (EPS), the rhizosphere develops a nutrient-rich and hydrating biofilm, creating an optimised and resilient microhabitat for root growth [11, 84, 85]. In addition to this role of mung bean mucilage in biological processes in the rhizosphere, it is also expected to play a significant role in physicochemical aspects of the rhizosphere, such as the interplay of physics, chemistry and biology has been highlighted recently [86]. In the following discussion, we describe the physicochemical role of mung bean mucilage in addition to the biological role so far.

The presence of low-methoxy pectin plays a primary role in various physicochemical properties such as viscosity, surface tension, wetting characteristics, and hydration capacity of the mucilage, which are important in the root-soil interactions. Low-methoxy pectins are known to form gels in the presence of divalent cations with varying mechanical and structural properties depending on the pectin and the ion concentrations and ratios. This contributes to the structural and functional role of mucilage in plants. The presence of cellulose, hemicellulose, and lipids in smaller quantities was also confirmed from the FTIR analysis. Cellulose shows well-defined absorption bands in 3500 to 2800 cm^{-1}, and 1740 to 600 cm^{-1}. However, the lower intensity of these peaks in the FTIR spectra of mung bean root mucilage suggests that cellulose and hemicellulose are minor components in the mucilage. FT-Raman and ^{1}H-NMR spectroscopy analyses also reinforce that low-methoxy pectin is the dominant structural component in the mung bean root mucilage, along with minor amounts of cellulose, hemicellulose, and lipids. The distribution of cellulose and pectin domains within the mung bean root mucilage is also confirmed through selective staining using ruthenium red (for pectin) and methylene blue (for cellulose). In optical microscopy, cellulosic

regions are observed in the boundaries of the border cells, whereas pectins are found primarily in the mucilage matrix and within the border cell interiors. Fresh mung bean root mucilage shows lower surface tension compared to water, which enables it to spread and wet the soil more easily. This helps form cohesive layers of soil, as can be observed from Fig. 8. The larger diameter of the soil blob adhering to the root tip with fresh mucilage (in comparison to the semi-dried mucilage on the root tip) shows a larger "sphere of wetting" of the mucilage in the soil. As the mucilage dries, this diameter reduces. In the previous section on physico-chemical characterisation, the presence of LM pectin and divalent ions, specifically calcium ions (Ca^{2+}) and magnesium ions (Mg^{2+}) was confirmed. These observations carry significant implications, as these divalent ions have the capacity to form crosslinks in the pectin molecules present in the mucilage, forming hydrogels. Gelation of the homogalacturonan region of LM pectin facilitated by calcium ions through 'egg-box crosslinks' and 'single point crosslinks' results in a unique mechanical response as detailed in the oscillatory shear rheology studies reported in [51]. This three-dimensional gel-like network present in the mucilage is expected to impart higher viscosity, elasticity, and structural integrity to the mucilage under shear forces. In addition to being the reservoir of water, mucilage also acts as an interface between soil and root and helps in protecting it due to its yield stress characteristics and gel-like properties.

The steady shear, oscillatory shear, and temperature-dependent rheological characteristics of the fresh root mucilage show interesting features of its structure. A comparison of the freshly collected and the reconstituted root mucilage (Fig. 11A) shows that the reconstituted mucilage can be used for creating identical viscosity profiles as that of fresh mucilage. The surface tension of the reconstituted mucilage, however, is higher than that of fresh mucilage. The shear thinning response can be correlated to the 3D gel network between the pectin chains and the divalent Ca/Mg cations. These ionic crosslinks are necessary in the mucilage for its water-holding

capacity as well as to protect the root tip from shear forces. The root growth rate, ranging from 0.007 s^{-1} to 0.014 s^{-1}, can be compared with the low-shear regime in rheology. Within this range, the shear-thinning behaviour of the fresh root mucilage becomes particularly relevant. The shear-thinning nature of the root mucilage helps in lowering the viscosity with increasing shear rates, thereby facilitating root movement through the soil matrix. This adaptive rheological property of mucilage minimises mechanical resistance during root penetration while ensuring the mucilage retains its critical structure and functions. Frequency sweep experiments also indicate weak gel-like behaviour for the mucilage. However, an increase in temperature can weaken the H-bonds contributing to the gel network, which further contributes to a decrease in the viscosity with an increase in temperature. The water storage capacity is enhanced by the presence of Ca and Mg crosslinks in the pectin-based gel network. Mung bean root mucilage is also found to be thermally stable during the temperature cycles between 5 and 50 °C (Fig. 10C). Although a small increase in the modulus values above 40 °C indicates structural changes in the mucilage, these changes were found to be completely reversible during the cooling cycle between 50 to 5 °C. This indicates H-bond breaking and reformation [87] helps the root mucilage also to reverse the changes up to 50 °C. This may help the plants overcome thermal stresses in the root zone (rhizosphere) if the soil temperature does not exceed 50 °C. Further studies would be required if climate-related heating of the soil can surpass 50 °C.

5.1 Relevance to plant and rhizosphere

Mung bean is one of the important plant-based protein sources for the world. It is also a nitrogen-fixing legume that helps soil restore its nitrogen reserve. Hence, understanding its physiology and interactions with the soil through the exuded root mucilage is very crucial for the response of the plant to the changes in the immediate rhizosphere. The present study shows lower surface tension and higher viscosity

for freshly collected mung bean root mucilage in comparison to water. This is similar to the properties of maize root mucilage. The lower surface tension signifies the mild surfactant nature of the mucilage, which helps in weakening the attractive or cohesive forces at the interface between the mucilage and the surrounding soil medium. The lower surface tension of the mucilage helps to "wet" the soil particles more effectively and to reach a larger volume of soil in the root zone, which may enable more effective nutrient uptake. In addition, the mucilage helps to adhere and coat more soil particles around the root tip, creating a larger volume of soil contact with the root in the rhizosphere. The water contact angle on glass and Teflon surfaces indicates that both hydrophilic and hydrophobic contributions operate through root mucilage, and this is especially relevant since the rhizosphere contains both these components. The interfacial strength of the root with the rhizosphere is reinforced through these interactions. The root mucilage exhibits higher zero shear viscosity in comparison to water. However, the shear thinning nature and the yield stress characteristics imply that the mucilage works like a lubricant around the root tip, helping it navigate through the soil medium easily without fracture of the root tip. Even though the viscosity of the mucilage is higher than that of water, due to its lower surface tension, it spreads in the porous soil medium with less resistance. The estimated Ohnesorge number, Oh=0.7 (Oh $<$ 1) for mung bean root mucilage indicates the role of surface tension forces being helpful for the penetration of the viscous mucilage into the soil pores through shear thinning as well as capillary forces. The viscous hydrogel nature of the mucilage facilitates the formation of a cohesive mucilage film on the root tip, which enhances the retention of water around the root zone by countering capillary forces that drive desiccation. During dry cycles, the mucilage also affects the hydraulic conductivity in the rhizosphere by maintaining water bridges between soil particles, as highlighted in a previous study [88]. The soil stabilization can be observed from the dry-wet cycle studies conducted on the root with mucilage at various stages of drying. The shape of

the soil blob remains intact, indicating strong adhesion of the soil particles by the drying mucilage. This further supports the glueing effect of root mucilage in binding the soil particles as previously observed [89–92]. The stabilised rhizosheath structure has important implications for plant health, aiding in nutrient absorption, water retention, and overall root-soil interactions, contributing to the ability of the plant to thrive in its environment, particularly under dry environmental conditions. The thermal properties and the thermo-rheological response of the mucilage indicate the ability of the mucilage to withstand thermal stresses and mechanical stresses experienced in the rhizosphere.

6 Conclusion

Mung bean (*Vigna radiata*), being one of the important pulse crops grown in the tropical, arid regions, has been the subject of investigation for its growth, yield, chemical and functional properties of the seeds, etc.. However, there have not been any investigations on the root mucilage of mung beans to understand its role in the root-soil interface. We report for the first time the collection and physicochemical characterization of fresh mung bean root mucilage. The rheological (mechanical) characteristics of the freshly collected mung bean root mucilage show weak hydrogel behaviour originating from the LM pectin cross-linked gel network. The chemical analysis, along with EDX studies, showed the presence of galacturonic acid as well as cations such as (Ca^{2+}) and small amounts of (Mg^{2+}) in the mucilage. Mucilage also has small amounts of phospholipids, which contribute to its lower surface tension, and polysaccharides such as hemicellulose and cellulose originating from the border cells exuded along with the mucilage. The symbiotic association between mung bean and *Bradyrhizobium* supports the biological nitrogen fixation, a capability mostly absent in non-leguminous crops such as maize. Mung bean root mucilage plays a critical role in these interactions by offering pentose sugars preferred by *Bradyrhizobium*. Mung bean root mucilage

forms stable soil blob, whose size is governed by its hydration and rehydration capacity and adhesive interaction with soil particles. This mucilage-driven adhesion suggests soil aggregation under drying-wetting cycles in the rhizosphere. These results are also supported by the rheological and wetting properties of mung bean mucilage.

The mucilage shows significantly higher viscosity than that of water. The lower surface tension of the root mucilage helps in wetting the soil more effectively and spreading easily in the porous soil medium, although the viscosity is higher than that of water. The mucilage exhibits mild yield stress characteristics, indicating its ability to behave as a soft, viscoelastic solid-like material (gel), retaining its shape when a certain shear force is applied. This may help the mucilage in protecting the root tip during root penetration. The shear-thinning nature and the yield stress characteristics indicate the role of mucilage in providing effective lubrication during root growth. The response of the mucilage to thermal variations investigated using rheology indicated that the modulus of the mung bean root mucilage is stable between 5 and 50 °C. Maximum soil temperature recorded up to 5 cm depth during the hottest days in certain regions of India showed a maximum of 53 °C. This may increase further in the global warming and climate change scenario. Although mung bean root mucilage is stable up to 50 °C, it needs to be investigated further to understand how the root mucilage may affect plant survival under extreme climate conditions. Collectively, this work presents characteristics of a novel root mucilage and the effect of these characteristics on biological and physicochemical processes at the root-soil interface.

Acknowledgments

The Soil Testing Laboratory, Tamil Nadu Agricultural University (TNAU), is acknowledged for providing the soil samples used in the study.

Author contributions

Moumita Sasmal: Writing – original draft, Investigation, Formal analysis, Data curation. Abhijit P Deshpande and Susy Varughese: Conceptualisation, Writing– review and editing, Supervision.

Funding

The authors acknowledge the Science and Engineering Research Board (SERB), Government of India, for the funds received for this research work. CRG/2020/005288

Declaration of competing interest

The authors declare no conflict of interest.

Data availability

The data presented in the study are included in the article/Supplemental Material.

References

[1] Akale, A., Abdalla, M., Koehler, T., Sauer, A.M., Diamantopoulos, E., Ahmed, M.A.: Root mucilage enhances plant water use under combined soil and atmospheric drought. Annals of Botany **136**(5–6), 182 (2025) https://doi.org/10.1093/aob/mcaf182

[2] Ahmed, M.A., Holz, M., Woche, S.K., Bachmann, J., Carminati, A.: Effect of soil drying on mucilage exudation and its water repellency: a new method to collect mucilage. Journal of Plant Nutrition and Soil Science **178**(6), 821–824 (2015)

[3] Carminati, A., Moradi, A.B., Vetterlein, D., Vontobel, P., Lehmann, E., Weller, U., Vogel, H.-J., Oswald, S.E.: Dynamics of soil water content in the rhizosphere. Plant and soil **332**, 163–176 (2010)

[4] Bengough, A.G., McKenzie, B., Hallett, P., Valentine, T.: Root elongation, water stress, and mechanical impedance: a review of limiting stresses and beneficial root tip traits. Journal of experimental botany **62**(1), 59–68 (2011)

[5] Sievers, A., Braun, M., Monshausen, G.B.: The root cap: structure and function. In: Plant Roots, pp. 79–103. CRC Press, ??? (2002)

[6] Naveed, M., Brown, L., Raffan, A., George, T.S., Bengough, A.G., Roose, T., Sinclair, I., Koebernick, N., Cooper, L., Hackett, C.A., *et al.*: Plant exudates may stabilize or weaken soil depending on species, origin and time. European Journal of Soil Science **68**(6), 806–816 (2017)

[7] Kroener, E., Holz, M., Zarebanadkouki, M., Ahmed, M., Carminati, A.: Effects of mucilage on rhizosphere hydraulic functions depend on soil particle size. Vadose Zone Journal **17**(1), 1–11 (2018)

[8] Benard, P., Zarebanadkouki, M., Carminati, A.: Physics and hydraulics of the rhizosphere network. Journal of Plant Nutrition and Soil Science **182**(1), 5–8 (2019)

[9] Morel, J.L., Habib, L., Plantureux, S., Guckert, A.: Influence of maize root mucilage on soil aggregate stability. Plant and soil **136**, 111–119 (1991)

[10] Traoré, O., Groleau-Renaud, V., Plantureux, S., Tubeileh, A., Boeuf-Tremblay, V.: Effect of root mucilage and modelled root exudates on soil structure. European journal of soil science **51**(4), 575–581 (2000)

[11] Guhra, T., Stolze, K., Totsche, K.U.: Pathways of biogenically excreted organic matter into soil aggregates. Soil Biology and Biochemistry **164**, 108483 (2022)

[12] Mueller, C.W., Baumert, V., Carminati, A., Germon, A., Holz, M., Kögel-Knabner, I., Peth, S., Schlüter, S., Uteau, D., Vetterlein, D., *et al.*: From rhizosphere to detritusphere–soil structure formation driven by plant roots and the interactions with soil biota. Soil Biology and Biochemistry **193**, 109396 (2024)

[13] Bengough, A.G., Loades, K., McKenzie, B.M.: Root hairs aid soil penetration by anchoring the root surface to pore walls. Journal of Experimental Botany **67**(4), 1071–1078 (2016)

[14] Ahmed, M.A., Kroener, E., Benard, P., Zarebanadkouki, M., Kaestner, A., Carminati, A.: Drying of mucilage causes water repellency in the rhizosphere of maize: measurements and modelling. Plant and Soil **407**, 161–171 (2016)

[15] Benard, P., Zarebanadkouki, M., Hedwig, C., Holz, M., Ahmed, M.A., Carminati, A.: Pore-scale distribution of mucilage affecting water repellency in the rhizosphere. Vadose Zone Journal **17**(1), 1–9 (2018)

[16] Carminati, A., Vetterlein, D.: Plasticity of rhizosphere hydraulic properties as a key for efficient utilization of scarce resources. Annals of botany **112**(2), 277–290 (2013)

[17] Benizri, E., Nguyen, C., Piutti, S., Slezack-Deschaumes, S., Philippot, L.: Additions of maize root mucilage to soil changed the structure of the bacterial community. Soil biology and biochemistry **39**(5), 1230–1233 (2007)

[18] Ahmed, M.A., Sanaullah, M., Blagodatskaya, E., Mason-Jones, K., Jawad, H., Kuzyakov, Y., Dippold, M.A.: Soil microorganisms exhibit enzymatic and priming response to root mucilage under drought. Soil Biology and Biochemistry **116**, 410–418 (2018)

[19] Williams, K.A., Ruiz, S.A., Petroselli, C., Walker, N., Fletcher, D.M., Pileio, G., Roose, T.: Physical characterisation of chia mucilage polymeric gel and its implications on rhizosphere science-integrating imaging, mri, and modelling to gain insights into plant and microbial amended soils. Soil Biology and Biochemistry **162**, 108404 (2021)

[20] Matsuyama, T., Satoh, H., Yamada, Y., Hashimoto, T.: A maize glycine-rich protein is synthesized in the lateral root cap and accumulates in the mucilage. Plant Physiology **120**(3), 665–674 (1999)

[21] Guinel, F., McCully, M.: Some water-related physical properties of maize root-cap mucilage. Plant, Cell & Environment **9**(8), 657–666 (1986)

[22] Read, D., Gregory, P., Bell, A.: Physical properties of axenic maize root mucilage. Plant and Soil **211**, 87–91 (1999)

[23] Knott, M., Ani, M., Kroener, E., Diehl, D.: Effect of changing chemical environment on physical properties of maize root mucilage. Plant and Soil **478**(1),

85–101 (2022)

[24] Read, D., Gregory, P.: Surface tension and viscosity of axenic maize and lupin root mucilages. The New Phytologist **137**(4), 623–628 (1997)

[25] Ahmed, M.A., Zarebanadkouki, M., Ahmadi, K., Kroener, E., Kostka, S., Kaestner, A., Carminati, A.: Engineering rhizosphere hydraulics: pathways to improve plant adaptation to drought. Vadose Zone Journal **17**(1), 1–12 (2018)

[26] Naveed, M., Ahmed, M.A., Benard, P., Brown, L.K., George, T.S., Bengough, A., Roose, T., Koebernick, N., Hallett, P.: Surface tension, rheology and hydrophobicity of rhizodeposits and seed mucilage influence soil water retention and hysteresis. Plant and Soil **437**, 65–81 (2019)

[27] Affortit, P., Ahmed, M.A., Grondin, A., Delzon, S., Carminati, A., Laplaze, L.: Keep in touch: the soil–root hydraulic continuum and its role in drought resistance in crops. Journal of Experimental Botany **75**(2), 584–593 (2024)

[28] Brax, M., Buchmann, C., Kenngott, K., Schaumann, G.E., Diehl, D.: Influence of the physico-chemical properties of root mucilage and model substances on the microstructural stability of sand. Biogeochemistry **147**(1), 35–52 (2020)

[29] Amicucci, M.J., Galermo, A.G., Guerrero, A., Treves, G., Nandita, E., Kailemia, M.J., Higdon, S.M., Pozzo, T., Labavitch, J.M., Bennett, A.B., *et al.*: Strategy for structural elucidation of polysaccharides: elucidation of a maize mucilage that harbors diazotrophic bacteria. Analytical chemistry **91**(11), 7254–7265 (2019)

[30] Read, D.B., Bengough, A.G., Gregory, P.J., Crawford, J.W., Robinson, D., Scrimgeour, C., Young, I.M., Zhang, K., Zhang, X.: Plant roots release phospholipid surfactants that modify the physical and chemical properties of soil. New phytologist **157**(2), 315–326 (2003)

[31] Moradi, A.B., Carminati, A., Lamparter, A., Woche, S.K., Bachmann, J., Vetterlein, D., Vogel, H.-J., Oswald, S.E.: Is the rhizosphere temporarily water repellent? Vadose Zone Journal **11**(3), 2011–0120 (2012)

[32] Moradi, A.B., Carminati, A., Vetterlein, D., Vontobel, P., Lehmann, E., Weller, U., Hopmans, J.W., Vogel, H.-J., Oswald, S.E.: Three-dimensional visualization and quantification of water content in the rhizosphere. New Phytologist **192**(3), 653–663 (2011)

[33] McCully, M., Boyer, J.: The expansion of maize root-cap mucilage during hydration. 3. changes in water potential and water content. Physiologia Plantarum **99**(1), 169–177 (1997)

[34] Bengough, A., Kirby, J.: Tribology of the root cap in maize (zea mays) and peas (pisum sativum). The New Phytologist **142**(3), 421–425 (1999)

[35] Iijima, M., Higuchi, T., Barlow, P.W., Bengough, A.G.: Root cap removal increases root penetration resistance in maize (zea mays l.). Journal of experimental botany **54**(390), 2105–2109 (2003)

[36] Archambault, D.J., Zhang, G., Taylor, G.J.: Accumulation of al in root mucilage of an al-resistant and an al-sensitive cultivar of wheat. Plant physiology **112**(4), 1471–1478 (1996)

[37] Werner, L.M., Knott, M., Diehl, D., Ahmed, M.A., Banfield, C., Dippold, M., Vetterlein, D., Wimmer, M.A.: Physico-chemical properties of maize (zea mays l.) mucilage differ with the collection system and corresponding root type and developmental stage of the plant. Plant and Soil **478**(1), 103–117 (2022)

[38] Nazari, M., Riebeling, S., Banfield, C.C., Akale, A., Crosta, M., Mason-Jones,

K., Dippold, M.A., Ahmed, M.A.: Mucilage polysaccharide composition and exudation in maize from contrasting climatic regions. Frontiers in plant science **11**, 587610 (2020)

[39] Xu, S., Li, X.-Q., Guo, H., Wu, X.-Y., Wang, N., Liu, Z.-Q., Hao, H.-Q., Jing, H.-C.: Mucilage secretion by aerial roots in sorghum (sorghum bicolor): sugar profile, genetic diversity, gwas and transcriptomic analysis. Plant molecular biology **112**(6), 309–323 (2023)

[40] Pankievicz, V.C.S., Delaux, P.-M., Infante, V., Hirsch, H.H., Rajasekar, S., Zamora, P., Jayaraman, D., Calderon, C.I., Bennett, A., Ané, J.-M.: Nitrogen fixation and mucilage production on maize aerial roots is controlled by aerial root development and border cell functions. Frontiers in plant science **13**, 977056 (2022)

[41] Abbas, S., Javed, M.T., Shahid, M., Tanwir, K., Saleem, M.H., Niazi, N.K.: Deciphering the impact of acinetobacter sp. sg-5 strain on two contrasting zea mays l. cultivars for root exudations and distinct physio-biochemical attributes under cadmium stress. Journal of Plant Growth Regulation **42**(11), 6951–6968 (2023)

[42] Higdon, S.M., Pozzo, T., Kong, N., Huang, B.C., Yang, M.L., Jeannotte, R., Brown, C.T., Bennett, A.B., Weimer, B.C.: Genomic characterization of a diazotrophic microbiota associated with maize aerial root mucilage. PloS one **15**(9), 0239677 (2020)

[43] Wang, L., Rengel, Z., Zhang, K., Jin, K., Lyu, Y., Zhang, L., Cheng, L., Zhang, F., Shen, J.: Ensuring future food security and resource sustainability: insights into the rhizosphere. Iscience **25**(4), 104168 (2022)

[44] Sun, H., Jiang, S., Jiang, C., Wu, C., Gao, M., Wang, Q.: A review of root

exudates and rhizosphere microbiome for crop production. Environmental Science and Pollution Research **28**(39), 54497–54510 (2021)

[45] Jimenez-Lopez, J.C., Singh, K.B., Clemente, A., Nelson, M.N., Ochatt, S., Smith, P.M.: Legumes for global food security. Frontiers Media SA (2020)

[46] Pannu, R., Singh, D.: Effect of irrigation on water use, water-use efficiency, growth and yield of mungbean. Field Crops Research **31**(1-2), 87–100 (1993)

[47] Sengupta, K.: Mung bean (green gram). In: Forage Crops of the World, Volume II: Minor Forage Crops, pp. 159–174. Apple Academic Press, ??? (2018)

[48] Adsule, R., Kadam, S., Salunkhe, D., Luh, B.: Chemistry and technology of green gram (vigna radiata [l.] wilczek). Critical Reviews in Food Science & Nutrition **25**(1), 73–105 (1986)

[49] Priya, M., Bhardwaj, A., Jha, U.C., HanumanthaRao, B., Prasad, P.V., Sharma, K.D., Siddique, K.H., Nayyar, H.: Investigating the influence of elevated temperature on nutritional and yield characteristics of mung bean (vigna radiata l.) genotypes during seed filling in a controlled environment. Frontiers in Plant Science **14**, 1233954 (2023)

[50] Holz, M., Leue, M., Ahmed, M.A., Benard, P., Gerke, H.H., Carminati, A.: Spatial distribution of mucilage in the rhizosphere measured with infrared spectroscopy. Frontiers in Environmental Science **6**, 87 (2018)

[51] John, J., Ray, D., Aswal, V.K., Deshpande, A.P., Varughese, S.: Dissipation and strain-stiffening behavior of pectin–ca gels under laos. Soft Matter **15**(34), 6852–6866 (2019)

[52] Martín, C.d.M.G., Ramírez, O., Bonardd, S., López-Darias, M., Franco, L.,

M'Rabet, Y., Khwaldia, K., Díaz, D.D.: Unlocking the potential of opuntia species mucilage in chemistry. International journal of biological macromolecules **268**, 131647 (2024)

[53] Anselmucci, F., Andò, E., Viggiani, G., Lenoir, N., Arson, C., Sibille, L.: Imaging local soil kinematics during the first days of maize root growth in sand. Scientific reports **11**(1), 22262 (2021)

[54] Griffiths, J.S., North, H.M.: Sticking to cellulose: exploiting arabidopsis seed coat mucilage to understand cellulose biosynthesis and cell wall polysaccharide interactions. New Phytologist **214**(3), 959–966 (2017)

[55] Castilleux, R., Plancot, B., Ropitaux, M., Carreras, A., Leprince, J., Boulogne, I., Follet-Gueye, M.-L., Popper, Z.A., Driouich, A., Vicré, M.: Cell wall extensins in root–microbe interactions and root secretions. Journal of Experimental Botany **69**(18), 4235–4247 (2018)

[56] Szeghalmi, A., Kaminskyj, S., Gough, K.M.: A synchrotron ftir microspectroscopy investigation of fungal hyphae grown under optimal and stressed conditions. Analytical and bioanalytical chemistry **387**, 1779–1789 (2007)

[57] El-Sakhawy, M., Kamel, S., Salama, A., Tohamy, H.-A.S.: Preparation and infrared study of cellulose based amphiphilic materials. Cellul. Chem. Technol **52**(3-4), 193–200 (2018)

[58] Szymanska-Chargot, M., Zdunek, A.: Use of ft-ir spectra and pca to the bulk characterization of cell wall residues of fruits and vegetables along a fraction process. Food biophysics **8**, 29–42 (2013)

[59] Yu, H., Wang, J., Yu, J.-x., Wang, Y., Chi, R.-a.: Effects of surface modification on heavy metal adsorption performance and stability of peanut shell and

its extracts of cellulose, lignin, and hemicellulose. Environmental Science and Pollution Research **27**, 26502–26510 (2020)

[60] Moharram, M., Mahmoud, O.M.: Ftir spectroscopic study of the effect of microwave heating on the transformation of cellulose i into cellulose ii during mercerization. Journal of Applied Polymer Science **107**(1), 30–36 (2008)

[61] Focher, B., Palma, M., Canetti, M., Torri, G., Cosentino, C., Gastaldi, G.: Structural differences between non-wood plant celluloses: evidence from solid state nmr, vibrational spectroscopy and x-ray diffractometry. Industrial Crops and Products **13**(3), 193–208 (2001)

[62] Priya, V., Shrama, P., Kumar, A.: Phytoremediation of banana leaf-functionalization of mercaptan-cellulose and its utilization for the removal of heavy metals in aqueous environment. Asian J. Adv. Basic Sci **8**(1), 26–38 (2020)

[63] Synytsya, A., Čopíková, J., Matějka, P., Machovič, V.: Fourier transform raman and infrared spectroscopy of pectins. Carbohydrate Polymers **54**(1), 97–106 (2003)

[64] Chylińska, M., Szymańska-Chargot, M., Zdunek, A.: Ft-ir and ft-raman characterization of non-cellulosic polysaccharides fractions isolated from plant cell wall. Carbohydrate polymers **154**, 48–54 (2016)

[65] Bernardino-Nicanor, A., Montañez-Soto, J.L., Conde-Barajas, E., Negrete-Rodríguez, M.d.l.L.X., Teniente-Martínez, G., Vargas-León, E.A., Juárez-Goiz, J.M.S., Acosta-García, G., González-Cruz, L.: Spectroscopic and structural analyses of opuntia robusta mucilage and its potential as an edible coating. Coatings **8**(12), 466 (2018)

[66] Giancaspro, J., Scollan, P., Rosario, J., Miller, E., Braziel, S., Lee, S.: Structural

determination of model phospholipid membranes by raman spectroscopy: Laboratory experiment. Biochemistry and Molecular Biology Education **50**(2), 181–192 (2022)

[67] Ma, X., Pawlik, M.: Intrinsic viscosities and huggins constants of guar gum in alkali metal chloride solutions. Carbohydrate Polymers **70**(1), 15–24 (2007)

[68] Singh, S., Bothara, S.B.: Physico-chemical and structural characterization of mucilage isolated from seeds of diospyros melonoxylon roxb. Brazilian Journal of Pharmaceutical Sciences **50**(4), 713–725 (2014)

[69] Sáenz, C., Sepúlveda, E., Matsuhiro, B.: Opuntia spp mucilage's: a functional component with industrial perspectives. Journal of arid environments **57**(3), 275–290 (2004)

[70] Reyes-Ocampo, I., Córdova-Aguilar, M., Guzmán, G., Blancas-Cabrera, A., Ascanio, G.: Solvent-free mechanical extraction of opuntia ficus-indica mucilage. Journal of Food Process Engineering **42**(1), 12954 (2019)

[71] Ray, T., Callow, J., Kennedy, J.: Composition of root mucilage polysaccharides from lepidium sativum. Journal of Experimental Botany **39**(9), 1249–1261 (1988)

[72] Amitrano, C., Arena, C., De Pascale, S., De Micco, V.: Light and low relative humidity increase antioxidants content in mung bean (vigna radiata l.) sprouts. Plants **9**(9), 1093 (2020)

[73] Ganeshi, N.G., Mujumdar, M., Takaya, Y., Goswami, M.M., Singh, B.B., Krishnan, R., Terao, T.: Soil moisture revamps the temperature extremes in a warming climate over india. npj Climate and Atmospheric Science **6**(1), 12 (2023)

[74] Capitani, M.I., Corzo-Rios, L.J., Chel-Guerrero, L., Betancur-Ancona, D.,

Nolasco, S.M., Tomás, M.C.: Rheological properties of aqueous dispersions of chia (salvia hispanica l.) mucilage. Journal of food engineering **149**, 70–77 (2015)

[75] Naji-Tabasi, S., Razavi, S.M.A.: New studies on basil (ocimum bacilicum l.) seed gum: Part ii—emulsifying and foaming characterization. Carbohydrate polymers **149**, 140–150 (2016)

[76] Bertsch, P., Diba, M., Mooney, D.J., Leeuwenburgh, S.C.: Self-healing injectable hydrogels for tissue regeneration. Chemical Reviews **123**(2), 834–873 (2022)

[77] Chu, Y., Zhao, Z., Schreiber, S., Zeng, H., Chen, L.: Size-controllable and ph-sensitive whey protein microgels as high-performance aqueous biolubricants. ACS Applied Materials & Interfaces **16**(35), 46909–46922 (2024) https://doi.org/10.1021/acsami.4c09771

[78] Martínez-Padilla, L.P.: Rheology of liquid foods under shear flow conditions: Recently used models. Journal of Texture Studies **55**(1), 12802 (2024)

[79] Nazari, M., Bilyera, N., Banfield, C.C., Mason-Jones, K., Zarebanadkouki, M., Munene, R., Dippold, M.A.: Soil, climate, and variety impact on quantity and quality of maize root mucilage exudation. Plant and Soil **482**(1), 25–38 (2023)

[80] Favero, V.O., Carvalho, R.H., Motta, V.M., Leite, A.B.C., Coelho, M.R.R., Xavier, G.R., Rumjanek, N.G., Urquiaga, S.: Bradyrhizobium as the only rhizobial inhabitant of mung bean (vigna radiata) nodules in tropical soils: A strategy based on microbiome for improving biological nitrogen fixation using bio-products. Frontiers in Plant Science **11**, 602645 (2021)

[81] Sosa-Saavedra, F., León-Barrios, M., Pérez-Galdona, R.: Pentose phosphate pathway as the main route for hexose catabolism in bradyrhizobium sp. lacking entner–doudoroff pathway. a role for nad+-dependent 6-phosphogluconate

dehydrogenase (decarboxylating). Soil Biology and Biochemistry **33**(3), 339–343 (2001)

[82] Salminen, S.O., Streeter, J.G.: Uptake and metabolism of carbohydrates by bradyrhizobium japonicum bacteroids. Plant physiology **83**(3), 535–540 (1987)

[83] Van Deynze, A., Zamora, P., Delaux, P.-M., Heitmann, C., Jayaraman, D., Rajasekar, S., Graham, D., Maeda, J., Gibson, D., Schwartz, K.D., *et al.*: Nitrogen fixation in a landrace of maize is supported by a mucilage-associated diazotrophic microbiota. PLoS biology **16**(8), 2006352 (2018)

[84] Kuzyakov, Y., Razavi, B.S.: Rhizosphere size and shape: temporal dynamics and spatial stationarity. Soil Biology and Biochemistry **135**, 343–360 (2019)

[85] Nazari, M., Bickel, S., Benard, P., Mason-Jones, K., Carminati, A., Dippold, M.A.: Biogels in soils: plant mucilage as a biofilm matrix that shapes the rhizosphere microbial habitat. Frontiers in Plant Science **12**, 798992 (2022)

[86] Pelosi, C., Michel, E., Beltrame, P., Cazaurang, S., Bérard, A., Beudez, N., Cajot, F., Caurel, C., Serbource, C., Renault, P., *et al.*: How to integrate biology, physics and chemistry for a better description of soil water dynamics? Soil Biology and Biochemistry **214**, 110057 (2025)

[87] Yu, H., Xiao, Q., Qi, G., Chen, F., Tu, B., Zhang, S., Li, Y., Chen, Y., Yu, H., Duan, P.: A hydrogen bonds-crosslinked hydrogels with self-healing and adhesive properties for hemostatic. Frontiers in bioengineering and biotechnology **10**, 855013 (2022)

[88] Carminati, A., Benard, P., Ahmed, M.A., Zarebanadkouki, M.: Liquid bridges at the root-soil interface. Plant and Soil **417**, 1–15 (2017)

[89] Jastrow, J., Miller, R., Lussenhop, J.: Contributions of interacting biological mechanisms to soil aggregate stabilization in restored prairie. Soil Biology and Biochemistry **30**(7), 905–916 (1998)

[90] Totsche, K.U., Amelung, W., Gerzabek, M.H., Guggenberger, G., Klumpp, E., Knief, C., Lehndorff, E., Mikutta, R., Peth, S., Prechtel, A., *et al.*: Microaggregates in soils. Journal of Plant Nutrition and Soil Science **181**(1), 104–136 (2018)

[91] Poirier, V., Roumet, C., Munson, A.D.: The root of the matter: Linking root traits and soil organic matter stabilization processes. Soil Biology and Biochemistry **120**, 246–259 (2018)

[92] Wang, X., Sale, P., Hayden, H., Tang, C., Clark, G., Armstrong, R.: Plant roots and deep-banded nutrient-rich amendments influence aggregation and dispersion in a dispersive clay subsoil. Soil Biology and Biochemistry **141**, 107664 (2020)

Supplementary Files

This is a list of supplementary files associated with this preprint. Click to download.

- S1.jpg
- S2.jpg
- S3.jpg
- S4.jpg
- S5.jpg